Wiley
Journal of Food Biochemistry
Volume 2025, Article ID 8543663, 24 pages
https://doi.org/10.1155/jfbc/8543663

WILEY

Research Article

Deciphering the Molecular Pathways: How *Polygonatum sibiricum* Alleviates Myocardial Ischemia

Zhenzhong Zhu,[1] **Junzhi Pan**,[2] **Bin Jiang**,[3] **Yuanlong Zhang**,[3] **Yanxia Lv**,[4] **Yifan Pan**,[1] **Yunxiang Wang**,[1] **and Weijun Lv**[1]

[1]*Department of Vasculocardiology, Yongkang First People's Hospital Affiliated to Hangzhou Medical College, Yongkang 321300, China*
[2]*Department of Emergency, Yongkang First People's Hospital Affiliated to Hangzhou Medical College, Yongkang 321300, China*
[3]*School of Pharmaceutical Sciences, Wenzhou Medical University, Wenzhou 325035, China*
[4]*Department of Pharmacy, Yongkang First People's Hospital Affiliated to Hangzhou Medical College, Yongkang 321300, China*

Correspondence should be addressed to Yunxiang Wang; wangyunxiang@hmc.edu.cn and Weijun Lv; 13868955410@163.com

Received 15 October 2023; Revised 23 December 2024; Accepted 11 March 2025

Academic Editor: Snehasis Chakraborty

Copyright © 2025 Zhenzhong Zhu et al. Journal of Food Biochemistry published by John Wiley & Sons Ltd. This is an open access article under the terms of the Creative Commons Attribution License, which permits use, distribution and reproduction in any medium, provided the original work is properly cited.

Herbal medicine, like *Polygonatum sibiricum*, is gaining attention for its potential in treating myocardial ischemia. Comprehensive research on its molecular interplay is essential for its development as a therapeutic agent. The aim is to investigate the molecular mechanisms by which *Polygonatum sibiricum* ameliorates myocardial ischemia. The study involves a thorough database exploration, molecular docking, and the use of both in vivo and in vitro models for detailed assessment. The role of the HIF-1α pathway is particularly emphasized. Identification of 11 principal components and 23 core proteins, with a dominant role of HIF-1α, was achieved. A notable improvement in myocardial conditions, attributable to *Polygonatum sibiricum*, was observed. *Polygonatum sibiricum* improves myocardial ischemic injury by augmenting mitochondrial activity and enhancing the HIF-1α pathway.

Keywords: HIF-1α; mitochondria; molecular docking verification; molecular mechanism; myocardial ischemia; *Polygonatum sibiricum*; UPLC-Q/TOF/MS

1. Introduction

Myocardial ischemic injury is a significant cardiovascular disease that has a profound impact on patients and cannot be disregarded [1]. The main challenge in treating this condition is the imbalance between oxygen supply and demand in myocardial cells, necessitating immediate intervention to prevent myocardial necrosis [2]. Nevertheless, despite timely treatment, patients generally have a bleak prognosis, since myocardial ischemia (MI) can result in severe complications including myocardial infarction and heart failure [3].

Cardiovascular disease poses a significant health challenge worldwide, and traditional Chinese medicine presents a promising treatment approach [4]. In particular, *Polygonatum sibiricum* has been found to possess several beneficial biological activities for maintaining cardiovascular health [5]. *Polygonatum sibiricum* has the potential to stabilize coronary arteries, alleviate cardiac stress, and lower the risk of cardiovascular disease [6]. Furthermore, it can additionally combat cardiovascular diseases through mechanisms such as antioxidation and lipid reduction [7]. The characteristics of this plant highlight its potential significance in managing cardiovascular health and guiding future research and development [8]. In the future, *Polygonatum sibiricum* could potentially see expanded usage as an adjuvant treatment and preventative measure for cardiovascular diseases [9].

Protecting mitochondria has a significant impact on improving myocardial ischemic injury [10]. The proper functioning of the heart relies on the optimal condition of mitochondria since they act as the primary energy source for

cardiac cells [11]. Ensuring proper mitochondrial function helps prevent or alleviate various complications arising from MI. Additionally, it can enhance the overall efficacy of heart disease treatment and contribute to patients' potential for recovery [12].

The research conclusion indicates that *Polygonatum sibiricum*, a Chinese medicinal herb, can safeguard mitochondrial function by activating the HIF-1α pathway. This finding establishes novel treatment targets and highlights the potential therapeutic value of *Polygonatum sibiricum* in managing myocardial ischemic injury. This finding suggests that *Polygonatum sibiricum* could be used as a drug for treating cardiovascular diseases. It is believed to improve mitochondrial function in cardiac cells, thereby alleviating damage and offering improved treatment options for patients.

2. Materials and Methods

2.1. Active Ingredients and Target Screening of Rhizoma Polygonati. The active chemical components of *Polygonatum sibiricum* were screened using three databases: the HERB database (https://herb.ac.cn/), TCMSP database (https://old.tcmsp-e.com/tcmsp.php), and BATMAN-TCM database (https://bionet.ncpsb.org.cn/batman-tcm/). The keyword "*Polygonatum sibiricum*" was used for the screening process. In the HERB database, Lipinski's five rules (MW ≦ 500, miLogP ≦ 5, nOHNH ≦ 5, and nOH ≦ 10) were employed as screening criteria. In the TCMSP database, oral bioavailability (OB > 30%) and drug-likeness (DL > 0.18) were used as the screening parameters. In the BATMAN-TCM database, Score > 20 and adjusted p_value < 0.05 were adopted as criteria to select representative chemical constituents of *Polygonatum sibiricum*. The resulting samples were analyzed using the SwissTargetPrediction database (https://www.swisstargetprediction.ch/) after nontargeted components and duplicate active ingredients were removed. Targets for these active compounds were determined by setting the threshold to the top 15 [13, 14]. The selection of the threshold (top 15) is based on the design principles of the SwissTargetPrediction database, which are determined by the algorithm's predictive accuracy and actual test results [15].

2.2. Collection of Targets Related to MI. To identify target genes associated with MI, searches were conducted in the DISGeNET database (https://www.disgenet.org/), the OMIM database (https://omim.org/), and the GeneCards database (https://www.genecards.org/) using the keyword "Myocardial Ischemia". The retrieved target genes were integrated, and duplicate values were removed [16].

2.3. This Study Aims to Identify Potential Targets for Polygonatum sibiricum in the Treatment of MI. The potential target genes associated with the active compounds in *Polygonatum sibiricum* were matched with relevant target genes for MI using R language (R version 3.6.3). This process enabled the identification of overlapping genes between the two sets, indicating potential target genes for *Polygonatum sibiricum* in the treatment of MI. A Venn diagram illustrating the intersection of these genes was generated.

2.4. Development of the Potential Target Network for Polygonatum sibiricum (Rhizoma Polygonati) and Its Active Ingredients in MI. Cytoscape 3.8.2 software was employed to construct a network revealing the correspondence between *Polygonatum sibiricum*, MI, active ingredients, and potential target sites. The constructed network was subsequently subjected to topological analysis. Nodes with higher degree values were identified as indicating greater effectiveness of the corresponding active ingredients [16].

2.5. The Construction of Protein–Protein Interaction (PPI) Networks and the Screening of Core Targets. The potential targets of *Polygonatum sibiricum* in the treatment of MI were imported into the STRING online database (https://string-db.org/). The species was set as *Homo sapiens*, the confidence score was set to ≥ 0.4, and free targets were hidden to construct the PPI network of potential targets. PPI network data were imported into Cytoscape software (version 3.8.2) for topological analysis. The CytoHubba plugin was utilized to filter core targets based on their node degree.

2.6. Gene Ontology (GO) Functional Enrichment Analysis and Kyoto Encyclopedia of Genes and Genomes (KEGG) Signal Pathway Analysis. GO enrichment and KEGG pathway enrichment analyses were conducted on the obtained core target genes using the Bioconductor platform and R language. A significance cutoff of $p < 0.05$ was applied. GO enrichment analysis encompasses analyses of biological process (BP), molecular function (MF), and cellular component (CC), ultimately unveiling the major cellular functions and signaling pathways affected by the core targets [17].

2.7. Molecular Docking. The molecular docking was performed using the selected core targets and the target compounds with high degree values. The crystal structures of the core proteins were downloaded from the Protein Data Bank [18]. The structures of the active compound compounds were obtained from the PubChem database and converted into three-dimensional structures using Chem3DUltra 14.0 software, followed by energy minimization using the MM2 algorithm. The target protein receptor, ERK, was prepared using PyMOL software by dehydrating and removing organic molecules. The target protein receptor molecules were then processed for hydrogenation and charge calculation using AutoDockTools 1.5.6. The compound and target protein receptor were converted into pdbqt files, and appropriate box centers and grid parameters were set. Finally, Vina 1.1.2 was executed to evaluate the molecular docking and calculate the docking energy values [19].

2.8. Animal Testing Drug Formulation. Polygonatum sibiricum was obtained from Beijing Putian Tongchuang Biotechnology Co., Ltd (Batch number: 121341-201705) and identified as *Polygonatum sibiricum* (*Polygonatum cyrtonema Hua.*), a plant belonging to the Liliaceae family. The dried rhizomes were used for the study. The ethanol extract of

Polygonatum sibiricum was prepared by soaking the plant material in 50% ethanol (sample to solvent ratio of 1:10, w/v) for 30 min, followed by a warm infusion (45°C) for 1 h. The mixture was then filtered, and the residue was subjected to a second warm infusion using distilled water at 45°C for 1 h. The resulting filtrate was collected using four layers of gauze, and the ethanol was completely removed by rotary evaporation. The obtained extract was concentrated into a thick paste, freeze-dried, and stored at −80°C for further use [20]. For the animal experiments, the freeze-dried powder of *Polygonatum sibiricum* was dissolved in water at a concentration of 2 g/mL. The doses were calculated using the equivalent dose conversion method from the book "Pharmacological Experimental Methodology" edited by Professor Xu Shuyun. The oral dose for adults was 0.3 g/kg/day, and for rats, the oral dose was 2 g/kg/day. The low and high doses were set as 0.5 and 2 times the medium dose, respectively, resulting in animal doses of 1.0, 2.0, and 4.0 g/kg/day [21].

Isoproterenol (ISO), purchased from Sigma-Aldrich (6078-56-4, Sigma-Aldrich, Shanghai, China), was administered to the animals at 40 mg/kg/day. Compound Danshen Dripping Pills (CDDP) were purchased from Tasly Pharmaceutical Group Co., Ltd. (Batch number Z10950111, Tianjin, China) and administered to the animals at a dose of 73 mg/kg/day [22, 23].

2.9. High-Performance Liquid Chromatography-Tandem Mass Spectrometry (HPLC-MS/MS). Preparation of Plant Extract: Dry *Polygonatum sibiricum* rhizomes were ground into a fine powder. A quantity of 0.5 g of this powder was ultrasonically extracted with 10 mL methanol (MeOH) at room temperature for 1 h. The extract was evaporated and redissolved in 1.5 mL of MeOH, followed by the addition of 3.5 mL of water to make a 30% MeOH solution (5 mL total). Elution was conducted using 30% and 80% MeOH/H_2O solutions.

Standard solutions of neoliquiritin, digitalis glycoside, timosaponin, sibiricoside, and rhamnose were prepared at a concentration of 0.50 mg/mL in water to serve as controls.

HPLC-MS/MS analysis was performed using an LCMS-8040 triple quadrupole LC/MS/MS mass spectrometer equipped with a YMC-Triart C18 column (3.0 μm, 150 × 20 mm) maintained at 35°C. The flow rate was set at 0.2 mL/min, with 0.1% formic acid in water (A) and 0.1% formic acid in acetonitrile (B) as mobile phases. Gradient elution was carried out from 20% to 70% B over 40 min, followed by 100% B for 10 min. The column was equilibrated for 15 min prior to injection. A sample volume of 4 μL was injected for qualitative analysis.

Detection and Quantification: The mass spectrometer was operated in both positive and negative ion modes with a scan range of 100–1600 m/z. ESI parameters were set with an interface voltage of 4.5 kV (positive mode) and −3.5 kV (negative mode), a drying gas at 15 L/min, and a drying temperature of 350°C. Equal volumes of sample and standard solutions were analyzed to determine the content of active components by peak area comparison.

2.10. Construction and Grouping of Rat MI Model. Male Sprague Dawley (SD) rats, weighing 200–250 g and aged 8–9 weeks, were obtained from Beijing Weitonglihua Experimental Animal Technology Co., Ltd (Catalog number: 101, Beijing, China) and housed at a temperature of 23 ± 2°C and a relative humidity of 50 ± 10% under SPF conditions. The rats were given ad libitum access to water and fed a standard diet. The Institutional Animal Ethics Committee has approved the experimental protocol and animal use plan (NO. SCXK 2020-017). After 1 week of acclimation feeding, the rats were randomly assigned to six groups, with six rats in each group. These groups were the control group, model group (ISO), low-dose *Polygonatum sibiricum* group (DHJ + ISO), medium-dose *Polygonatum sibiricum* group (MHJ + ISO), high-dose *Polygonatum sibiricum* group (HHJ + ISO), and positive drug CDDP control group (CDDP + ISO).

The corresponding medication was administered via continuous gastric lavage for 7 days, with a lavage volume of 10 mL·kg^{-1}, once daily. On the sixth day, one hour after gastric lavage, all groups, except the control group, received an intraperitoneal injection of ISO (40 mg/kg/day) dissolved in physiological saline for two consecutive days. This injection was given to induce an acute MI model in rats. The control group was given an equivalent volume of physiological saline injection. Twenty-four hours after the final injection of ISO, all rats were anesthetized using intraperitoneal injection of sodium pentobarbital solution (50 mg/kg) (Cat. No: MERCK: P11011, Beijing Zhijie Fangyuan Technology Co., Ltd., Beijing, China). Blood samples were obtained from the abdominal aorta and then centrifuged at 3000 rpm for 15 min at 4°C. The resulting serum was collected for biochemical and metabolomics analysis. The rats were euthanized using a 5% sodium pentobarbital solution (150 mg/kg). Subsequently, the heart was extracted for pathological and biochemical studies [22].

2.11. Measurement of Cardiac Electrophysiological Parameters. After the final administration of drugs, rats were anesthetized with a sodium pentobarbital solution (50 mg/kg) intraperitoneally. Electrocardiogram (ECG) measurements of limb lead II were performed using the PowerLab system (ADInstruments Pty Ltd). Changes in the ST segment were recorded as indicators of rat cardiac activity [24].

2.12. Heart-to-Weight Ratio. Following the euthanasia of the rats, the hearts were collected and rinsed with physiological saline. Subsequently, the weight of the hearts was determined using a precise balance. The rats' weight was monitored daily throughout the entire experimental process [24].

2.13. Biochemical Analysis. The serum levels of the following were measured using automated standardization procedures (Roche Hitachi 917/747, Mannheim, Germany): creatine

kinase isoenzyme MB (CK-MB) (H197-1-1, Nanjing, China), cardiac troponin I (cTnI) (H149-2-1, Nanjing, China), aspartate transaminase (AST) (C010-2-1, Nanjing, China), lactate dehydrogenase (LDH) (A020-2-2, Nanjing, China), interleukin-1β (IL-1β) (H002-1-1, Nanjing, China), and tumor necrosis factor-α (TNF-α) (H052-1-1, Nanjing, China). Detection of oxidative stress-related indicators in myocardial tissue included superoxide dismutase (SOD) (A001-3-2, produced in Nanjing), malondialdehyde (MDA) (A003-3-1, produced in Nanjing), and glutathione (GSH) (A006-2-1, produced in Nanjing), among others [25, 26].

2.14. H&E Staining. Following dissection, the harvested heart was rinsed with precooled PBS, and any remaining moisture was gently absorbed using clean filter paper. The tissue was then fixed in 4% paraformaldehyde for at least 24 h. Subsequently, a gradient dehydration process was performed, followed by embedding the tissue in paraffin for sectioning. Sudan III staining was carried out as follows: To deparaffinize the tissue sections, the slices were subjected to the following sequence: xylene treatment for 10 min, absolute ethanol treatment for 5 min, 95% ethanol treatment for 5 min, 85% ethanol treatment for 5 min, 70% ethanol treatment for 5 min, and a final rinse with distilled water for 5 min. Staining was then performed by treating the sections with hematoxylin for 4 min, followed by a 10-min rinse under running tap water. Differentiation was achieved with a quick 3-s treatment using hydrochloric acid–ethanol solution, followed by another 10-min rinse with tap water to restore a blue coloration. The sections were subsequently treated with eosin for 25 s to 1 min. Finally, the slides were dehydrated, cleared, and mounted for examination and analysis under a microscope [24].

2.15. TTC Staining Is Employed for the Detection of the Area of Myocardial Infarction in Rats. The transverse heart slices, which were 2 mm thick, were incubated with 1% TTC dye (2273GR005, BioFroxx, Switzerland) at 37°C for 20 min. Subsequently, the slices were fixed using 4% paraformaldehyde. Normal cardiac tissue, which refers to non-infarcted areas, is characterized by a red appearance, whereas abnormal cardiac tissue, indicating infarcted areas, exhibits a light gray coloration. The heart sections were imaged using a camera, and the infarct size was measured using ImageJ 1.6 software [24].

2.16. Examination of Mitochondrial Morphology in Rat Myocardial Cells via Transmission Electron Microscopy. Samples were collected within 3 min after euthanizing the rats. Subsequently, the heart tissue was removed, washed, and sliced into 2 × 2 mm sections. These sections were fixed in electron microscopy fixative for 2 h at room temperature and subsequently stored and transported at 4°C. Subsequently, the cells were embedded in 1% agarose, dehydrated, and then sectioned into ultra-thin slices (70 nm thickness) using an ultramicrotome. Double staining was performed with 3% uranyl acetate–citrate, followed by staining with ethanol for slicing for 15 min. Images were captured in Japan using a Hitachi HT7700 transmission electron microscope [24].

2.17. Mitochondrial Enzyme Detection. Succinate dehydrogenase (SDH) and malate dehydrogenase (MDH) are essential enzymes in the mitochondria's tricarboxylic acid cycle, and their activity reflects mitochondrial function. Tissue samples were prepared by creating a 10% tissue homogenate using a physiological saline solution. The activity of mitochondrial enzymes was assessed using SDH (mlsw_E0558, mlBio, China) and MDH (JK-E2376, Crystal Antibio, China) assay kits as per the manufacturer's instructions [24].

2.18. TUNEL Technique for Detecting Apoptosis in Rat Cardiomyocytes. Apoptosis of rat cardiomyocytes was detected in situ by staining the sections using the TUNEL assay kit (11684817910, Roche, Switzerland) following the standard operational procedures. Following the staining process, five independent fields were randomly chosen on each slide and observed under an immunofluorescence microscope.

Photographs were captured to observe apoptosis of cardiomyocytes in the myocardial tissue of rats. The apoptosis rate (%) of rat cardiomyocytes in each group was calculated by dividing the number of TUNEL-positive cells in rat cardiomyocytes by the total number of cardiomyocytes and multiplying by 100% [24].

2.19. Cell Culture and Screening. H9c2 rat myocardial cells (catalog number BFN60804388) obtained from the Cell Bank of the Chinese Academy of Sciences were cultured in DMEM/high-glucose medium (catalog number SH30243.01, HyClone, Logan, Utah, USA). The culture medium was supplemented with 10% fetal bovine serum (catalog number 16140089, Gibco, NYC, USA) and 1% penicillin–streptomycin (catalog number 15070063, Gibco, NYC, USA) and incubated at 37°C in a humidified incubator with 5% CO_2. When the cell reaches 80% confluency, they were subjected to experimental treatments.

In the experiment, the optimal dosage of *Polygonatum sibiricum* was determined through a pre-experiment. The cell experiment was subsequently divided into three groups. The control group (Control) treated H9c2 cells with PBS (the same amount as ISO) for 24 h. The model group (ISO) exposed H9c2 cells to 50 μM ISO for 24 h. The *Polygonatum sibiricum* + ISO group (ISO + HJ) pretreated H9c2 cells with 2.0 mg/mL *Polygonatum sibiricum* for 1 h, followed by incubation with 50 μM ISO for 24 h [24].

2.20. MTT Assay. Each group of cells was inoculated into a 96-well culture plate at a density of 5×10^3 cells per well in 100 μL of medium containing 10% FBS. After H9c2 cells had fully adhered to the wall, they were treated with the corresponding drugs for 24 h. Subsequently, 20 μL of MTT solution (0.5 mg/mL) was added to each well and incubated

at 37°C and 5% CO_2 for 4 h. The cell supernatant was removed, and 200 μL of dimethyl sulfoxide (DMSO) was added to each well. The plate was placed on a low-speed shaker for 10 min, and the absorbance value (OD) at 490 nm was measured using an enzyme-linked immunosorbent assay (ELISA) reader. Each experimental setting consists of six parallel holes, independently repeated three times. For analysis, the relative proliferation rate compared to the control was utilized [24].

2.21. Cell Transfection. Cell transfection is categorized into the following groups: si-NC group (transfection sequence in cells: 5′-UAGCGACTAAACATCAATTT-3′), si-HIF1α-#1 group (transfection sequence in cells: 5′-CACAGGGAAAGCGAG TGGTTGGT-3′), and si-HIF1α-#2 group (transfection sequence in cells: 5′-GCUGUUCACUAAAGUGGAAUC-3′). Transfection was conducted using LipofectamineTM 3000 transfection reagent (L3000-008, Invitrogen, CA, USA). The silencing efficiency of these two si-HIF1α sequences was detected using Western blot after 48 h of transfection. All plasmids were obtained from Shanghai Hanheng Biotechnology Co., Ltd., in Shanghai, China. They were used at a concentration of 50 ng/mL [27–29].

2.22. Intracellular LDH Activity Detection. The rate at which LDH is released is employed to analyze the extent of cellular damage. Inoculate H9c2 cells into a 6-well plate at a density of 1×10^6 cells per well. Following a 24-h treatment of H9c2 cells with the respective drugs, LDH activity levels were quantified using the BCA method. The instructions provided in the reagent kit (A020-2-2, Nanjing Jiancheng) were followed for the quantification process [24].

2.23. ROS Detection. Fluorescent probes, such as DCFH-DA and DHE, were utilized to quantify the presence of reactive oxygen species (ROS) in cells. H9c2 cells were inoculated into a 6-well plate at a density of 1×10^6 cells per well. Following drug treatment, H9c2 cells were incubated with 10 μM DCFH-DA (S0033S, Beyotime, China) and 5 μM DHE (S0063, Beyotime, China) at 37°C in a dark environment for 30 min. The observation was conducted using a fluorescence microscope. After that, the relative fluorescence intensity was measured using ImageJ 1.6 software [24].

2.24. Analysis of Mitochondrial Membrane Potential. The mitochondrial membrane potential was evaluated using the provided method and the mitochondrial membrane potential assay kit (Rh123) (62669-70-9; Sigma-Aldrich, USA). H9c2 cells were seeded at a density of 1×10^6 cells per well on a 96-well plate. The cells were then treated with the appropriate drugs for 24 h, followed by incubation at 37°C in the dark for 30 min. Finally, the cells were washed twice with PBS. The staining conditions were observed using a fluorescence microscope, and the fluorescence intensity was measured using ImageJ 1.6 software [25].

2.25. Apoptosis Assay by Annexin V-FITC/PI Staining. The V-FITC/PI Cell Apoptosis Detection Kit (556547, BD Biosciences, NJ, USA) was utilized to detect apoptosis in H9c2 cells. Each group of cells (1×10^6 cells per well) was inoculated into a 6-well plate. After the H9c2 cells were incubated with the respective drug for 24 h, the cells were collected and stained in the dark at room temperature for 15 min. The staining solution contained 5 μL of V-FITC, a membrane-associated protein, and 10 μL of PI. Subsequently, flow cytometry analysis was conducted using the FACSCalibur flow cytometer (catalog number: 342973, USA BD) according to the manufacturer's instructions. The upper right quadrant corresponds to late apoptotic cells, while the lower right quadrant corresponds to early apoptotic cells [25].

2.26. Detection of Ca^{2+}. H9c2 cells were inoculated at a density of 1×10^6 cells per well into a 6-well plate. The cells underwent treatment with the respective medication for 24 h. Following that, they were stained in the dark at a temperature of 5°C for 1 h using 3 μM Fluo-3 AM (Sigma-Aldrich, USA, 46393). The fluorescence intensity of Fluo-3 was measured using a flow cytometer [25].

2.27. Western Blot. The heart tissue and cells were digested using RIPA lysis buffer (P0013B, Beyotime Biotechnology, Shanghai, China). Protein concentration was determined using the BCA method (P0010, Bi Yun Tian, Shanghai, China). The proteins were loaded onto a polyacrylamide gel and transferred onto a PVDF membrane (IPVH85R, Millipore, Darmstadt, Germany) using the wet transfer method.

The membranes were incubated with primary antibodies, including rabbit anti-Bcl-2 (ab196495, 1:1500, Abcam, UK), rabbit anti-HIF1α (SAB5701087, 1:2000, Sigma-Aldrich, USA), rabbit anti-HO-1 (ab68477, 1:10,000, Abcam, UK), rabbit anti-Bax (2772, 1:1000, Cell Signaling Technology, USA), rabbit anti-C-caspase-3 (9661, 1:1000, Cell Signaling Technology, USA), and rabbit anti-β-actin (AF5003, 1:5000, Beyotime, China), in 5% BSA at room temperature for 1 h. The membranes were then incubated overnight at 4°C.

Following the washing step, the slides were incubated with a goat anti-rabbit IgG secondary antibody conjugated with HRP (ab6721, 1:5000, Abcam, UK) for 2 h. The membrane was washed thrice with TBST for 5 min each, then detected using a chemiluminescence analyzer. Protein quantification analysis was conducted using ImageJ 1.6 software. Grayscale values of each protein were compared to the ratio of the internal control, β-actin, for protein quantification. Each experiment is repeated thrice [27, 30].

2.28. Based on UPLC-Q-TOF/MS Metabolomics Analysis. To extract serum, 100 μL of serum was mixed with 1000 μL of extraction solution (methanol: acetonitrile = 2:2:1, v/v) and vortexed thoroughly. The mixture was subjected to three cycles of continuous sonication in an ice bath for 10 min, followed by 1 min of liquid nitrogen exposure. Afterward,

the sample was incubated at −20°C for 1 h and centrifuged at 4°C and 3000 rpm for 15 min. The resulting supernatant was collected and dried using nitrogen blow at a purge flow rate of 15 L/min. Subsequently, 100 μL of a 50% acetonitrile–water solution (acetonitrile = 1:1, v/v) was added to the dried residue and vortexed for 30 s. The solution underwent 10 min of sonication in an ice bath, followed by centrifugation at 4°C and 3000 rpm for 15 min. The supernatant was collected and stored for further analysis.

Plasma metabolomic analysis was performed using a UPLC-Q-TOF/MS system (Agilent 1290 Infinity II LC, 6545 UHD Accurate-Mass Q-TOF/MS). Chromatographic analysis was conducted with a C18 column (2.1 × 100 mm, 1.8 μm; Agilent, USA). The injection volume was set to 5 μL, with the column maintained at 40°C, and the flow rate set at 0.4 mL/min. The mobile phase consisted of an aqueous solution containing acetonitrile and 0.1% formic acid. The gradient elution program initiated at 5% B for 2 min, gradually increasing from 5% B to 95% B over 12 min, and then maintaining 95% B for an additional 2 min.

For mass spectrometry, both positive and negative ion modes were applied. The ionization voltage was set at 5500 V, with a capillary temperature of 550°C, a spray gas flow rate of 50 psi, and an auxiliary heating gas flow rate of 60 psi. To prevent overfitting, orthogonal partial least squares discriminant analysis (OPLS-DA) was conducted alongside a 100-permutation test to analyze the preprocessed data. Metabolites were classified as differential metabolites (DMs) if they satisfied the conditions of a VIP score > 1 and a p-value < 0.05 in the OPLS-DA model. Furthermore, metabolites with a fold change ≥ 2 or ≤ 0.5 and a p-value < 0.05 in Student's t-test underwent univariate analysis and were designated as final DMs. Relevant metabolic pathways were identified using MetaboAnalyst [31, 32].

2.29. Principal Component Analysis (PCA) and OPLS-DA. OPLS-DA was conducted to further explore the potential mechanistic roles of *Polygonatum sibiricum* in the treatment of MI. Metabolomic data obtained from the HPLC-MS/MS experiments were normalized to minimize noise and eliminate interference, ensuring data accuracy and reliability.

Subsequently, PCA was performed using SIMCA-P 14.1 software. PCA, an unsupervised multivariate statistical method, reduced the dimensionality of high-dimensional data, transforming it into a lower dimensional space to reveal variations and group distributions within the dataset. Following PCA, OPLS-DA analysis was carried out using SIMCA-P 14.1 software. As a supervised multivariate statistical method, OPLS-DA segregated systematic variations within the data into classification-related and unrelated components, incorporating classification information to maximize intergroup differences. Model parameters were optimized, and model effectiveness was evaluated through cross-validation. Variable importance in projection (VIP) values were calculated to identify the metabolites contributing most significantly to group classification.

2.30. Statistical Analysis. Statistical analysis was performed using GraphPad Prism 9 software (GraphPad Software, USA) in this study. The measurement data are presented as the mean ± standard deviation. After assessing normality and equality of variances, a paired t-test is employed for between-group comparison if the data follow a normal distribution and exhibits equal variances. In cases involving multiple between-group comparisons, one-way analysis of variance or repeated measures analysis of variance is applied. A p value of less than 0.05 indicates statistical significance.

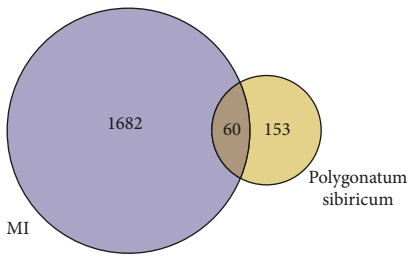
3. Results

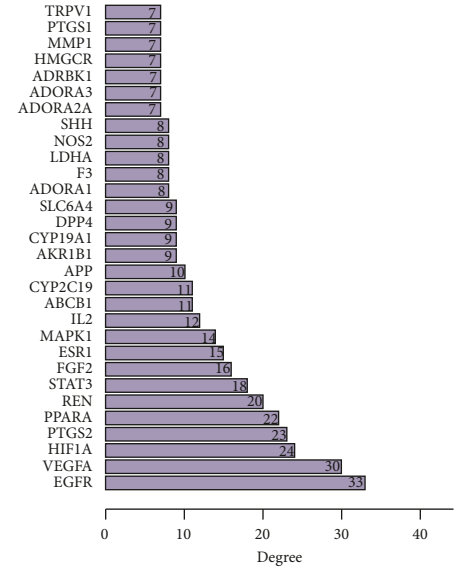
3.1. Multitarget Therapeutic Potential of Polygonatum sibiricum in MI: An Integrated Network Pharmacology Approach. To investigate potential targets of *Polygonatum sibiricum* for the treatment of MI, we retrieved the active chemical components of *Polygonatum sibiricum* from the HERB database, TCMSP database, and BATMAN-TCM database. Subsequently, we conducted a screening of these chemical components. A total of 21 active ingredients of *Polygonatum sibiricum* were identified in the HERB database, while in the TCMSP database and the BATMAN-TCM database, 8 and 5 active ingredients of *Polygonatum sibiricum* were identified, respectively. After eliminating duplicate entries from the filtered results of these three databases, we identified 31 chemical components of *Polygonatum sibiricum* (Table S1).

Next, we utilized the SwissTargetPrediction database to screen for target proteins corresponding to each compound, using a threshold of the top 15. This analysis yielded a total of 213 targets. The genes related to MI were sourced from the DISGeNET, OMIM, and GeneCards databases, yielding 756, 48, and 1165 target genes, respectively. After eliminating duplicates, 1742 MI-related target genes were acquired. We conducted a Venn analysis using R language to identify potential target genes associated with myocardial infarction for the active components of *Polygonatum sibiricum*. We obtained 60 overlapping target genes, as shown in Figure 1(a).

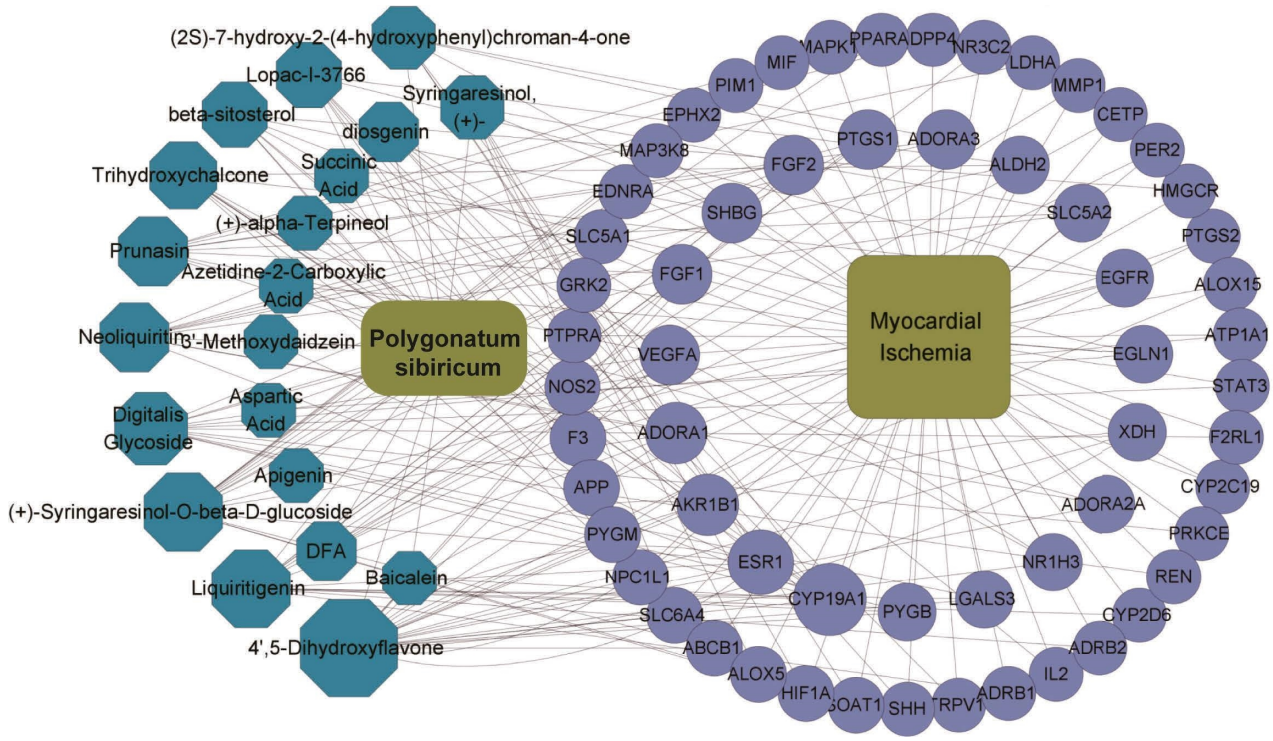
Subsequently, the active ingredients and overlapping targets were imported into Cytoscape 3.8.2 to construct a drug–ingredient–disease–target network for *Polygonatum sibiricum* treatment of MI (Figure 1(c)). After conducting network topology analysis, the median values of Betweenness, Closeness, and Degree for the compound were determined to be 0.009, 0.387, and 7, respectively. Among these compounds, 11 of them, namely, C2, C3, C5, C8, C15, C20, C21, C22, C25, C26, and C29, have the potential to interact with more than 7 targets, which suggests that they may serve as the primary active components in the treatment of MI with *Polygonatum sibiricum*. Moreover, we imported these 60 potential target genes into the STRING database to construct the PPI network (Figure 1(b); Figure 1(d)).

The core PPI network has been identified through topological analysis. We established filtering criteria for gene selection using the medians of Betweenness, Closeness, and Degree (0.005, 0.46, and 6.5, respectively) as thresholds. Ultimately, we identified 23 genes that play a crucial role in treating MI with *Polygonatum sibiricum*. These genes



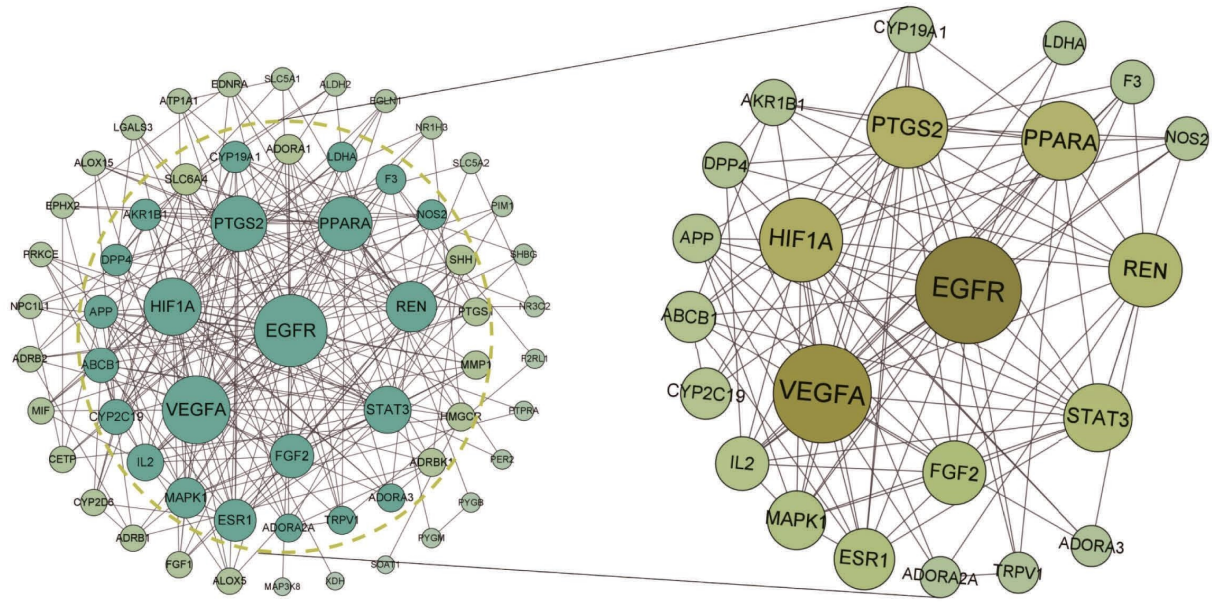


(a) (b)



(c)

Figure 1: Continued.



(d)

Figure 1: Potential targets and active ingredients of *Polygonatum sibiricum* for the treatment of myocardial ischemia. Note: (a) Venn diagram showing the potential targets in *Polygonatum sibiricum* involved in treating myocardial ischemia. (b) Interaction target frequency of the intersecting targets (Degree > 6.5). (c) Network diagram of the drug–ingredient–disease–target interactions for *Polygonatum sibiricum* in the treatment of myocardial ischemia, where green represents the active ingredients of *Polygonatum sibiricum* and blue represents the intersecting targets with myocardial ischemia. (d) PPI network analysis of the intersecting targets to identify core targets, with yellow indicating the core targets. The size of the circles represents the Degree values of the targets, with larger circles indicating higher Degree values.

represent the key targets in *Polygonatum sibiricum*'s treatment of MI.

Next, we conducted an enrichment analysis of GO and KEGG pathways on the identified 23 key target genes. Three categories of projects were identified in the GO results: 1318 BPs, 105 MFs, and 36 CCs. We visualized the top 10 pathways based on their p value (Figures 2(a) and 2(b)). The results of the KEGG analysis showed that these targets were enriched in a total of 65 pathways. We selected the top 20 pathways for visualization based on their p values (Figures 2(c) and 2(d)). These pathways include the HIF-1 signaling, relaxation, and VEGF signaling pathways, among others. These findings suggest that *Polygonatum sibiricum* contains multiple effective components that could exert their action on MI through various signal pathways.

The results above suggest that *Polygonatum sibiricum* exerts therapeutic effects on MI by coordinating multiple components and targets.

3.2. Molecular Docking Validates the Efficacy of Key Active Components in Polygonatum sibiricum for Targeting Core Pathways in MI. To validate the predicted results of network pharmacology, we chose the five most enriched pathways in the KEGG database and the 12 core targets with the highest Degree rankings as receptors. As ligands, we utilized 11 main active ingredients (Degree greater than 6.5) selected through drug–component–disease–target screening. The AutoDock Vina software validated molecular docking by docking 12 core targets with 11 major active compounds. When the binding energy is below 0 kJ/mol, it is understood that protein molecules bind and interact spontaneously. Moreover, lower binding energy contributes to a more stable molecular conformation [33].

The results of molecular docking (Figure 3(a); Table S2) indicate that the binding energies between the main active components and the core target range from $-2.3\,\text{kcal}\cdot\text{mol}^{-1}$ to $-11.4\,\text{kcal}\cdot\text{mol}^{-1}$, suggesting favorable binding activities between the main active components of *Polygonatum sibiricum* and the core target. The predicted results could be considered relatively reliable.

Seven docking complexes with relatively low binding energies (all less than −9 kJ/mol) were selected for visualization (Figures 3(b), 3(c), 3(d), 3(e), 3(f), 3(g), 3(h)). These seven docking combinations included MAPK1 with neoliquiritin, HIF-1α with neoliquiritin, CYP19A1 with digitalis glycoside, PPARA with digitalis glycoside, LDHA with digitalis glycoside, HIF-1α with digitalis glycoside, and EGFR with digitalis glycoside. It indicates that neoliquiritin and digitalis glycoside are critical components in *Polygonatum sibiricum*'s treatment of MI. Furthermore, HIF-1α could form stable conformations with neoliquiritin and digitalis glycoside, implying that HIF-1α may be a target for *Polygonatum sibiricum* in treating MI.

Furthermore, we conducted an analysis and identification of the chemical characteristics of *Polygonatum sibiricum* using HPLC-MS/MS. Specifically, dry rhizomes were ground into a fine powder, extracted with methanol, and analyzed using an LCMS-8040 triple quadrupole LC/MS/MS mass

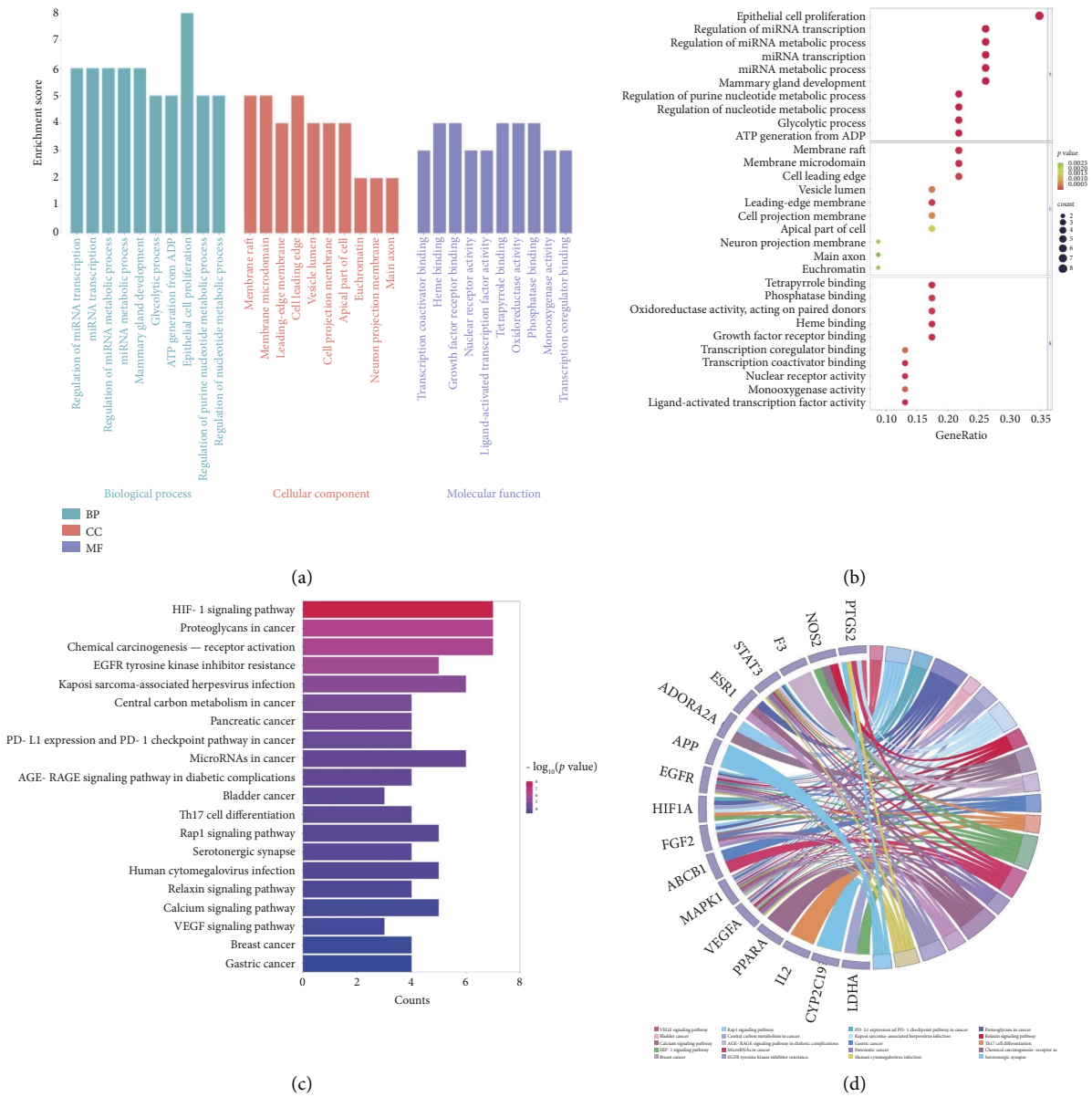
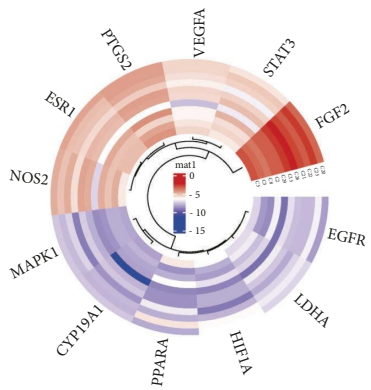


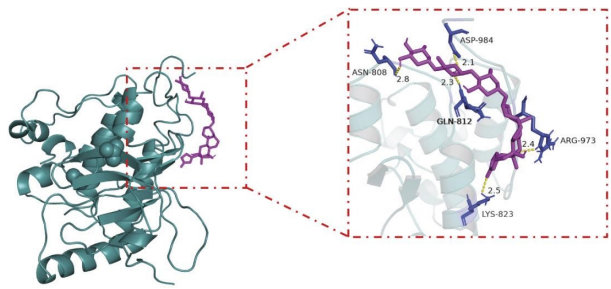
Figure 2: Bioinformatics analysis of key signaling pathways in treating myocardial ischemia with *Polygonatum sibiricum*. Note: (a) Bar graph showing GO functional annotation analysis of core targets. (b) Bubble graph showing GO functional annotation analysis of core targets. (c) Bar graph showing KEGG pathway enrichment analysis. (d) Circular graph showing KEGG enrichment analysis of core targets.

spectrometer with a YMC-Triart C18 column. The flow rate was set at 0.2 mL/min with gradient elution from 20% to 70% acetonitrile over 40 min, followed by 100% acetonitrile for 10 min. Detection was conducted in both positive and negative ion modes with a scan range of 100–1600 m/z, and the ESI parameters included an interface voltage of 4.5 kV (positive) and −3.5 kV (negative), a drying gas flow rate of 15 L/min, and a drying temperature of 350°C. The analysis revealed that neoliquiritin, digitalis glycoside, timosaponin, sibiricoside, and rhamnose are active components present in *Polygonatum sibiricum* (Figures S1A and S1B, Table S3). These mass spectrometry analysis results further validate that HIF-1α may be a key target for the treatment of MI using *Polygonatum sibiricum*.

3.3. Therapeutic Efficacy of Rhizoma Polygonati in Ameliorating ISO-Induced MI in Rats: Comparative Analysis With Positive Control Drug CDDP. To assess the therapeutic impact of Rhizoma Polygonati on MI, we induced a rat model of MI by intraperitoneally injecting ISO (Figure 4(a)). CDDP is a traditional Chinese medicine pill developed using modern, high-tech methods. It is notable for its stability, positive therapeutic effects, minimal adverse reactions, and ability to alleviate gastrointestinal irritation. CDDP is frequently employed in the treatment of ischemic heart disease. Numerous studies have corroborated the effects of CDDP, including the expansion of coronary arteries, increased blood flow, enhanced vascular smooth muscle cell function, and improved peripheral circulation. Thus, we selected CDDP as the positive drug for our study [22].

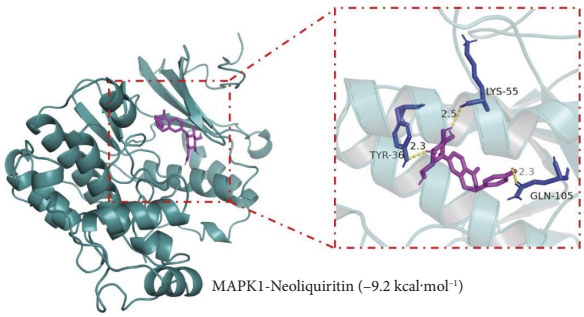


(a)



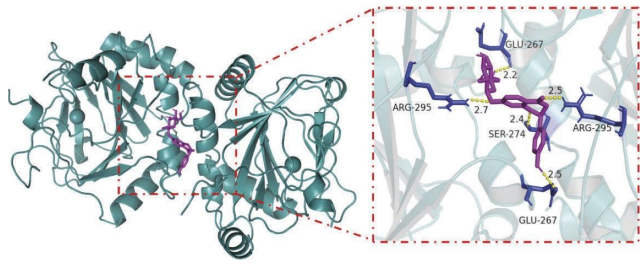
CYP19A1-Digitalis glycoside (−11.4 kcal·mol^{-1})

(b)



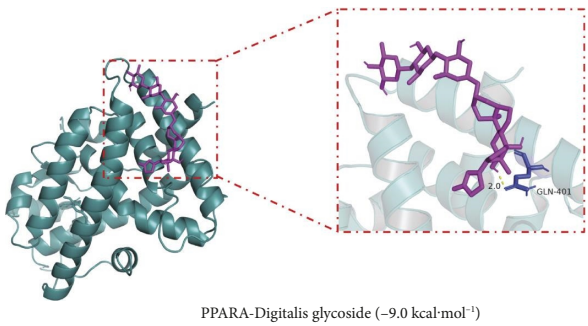
MAPK1-Neoliquiritin (−9.2 kcal·mol^{-1})

(c)



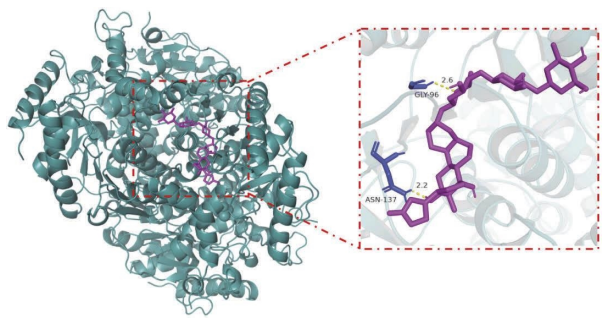
HIF1A-Neoliquiritin (−9.3 kcal·mol^{-1})

(d)



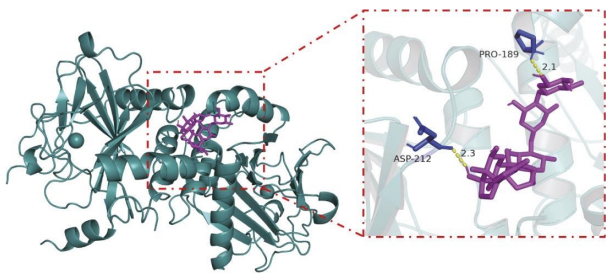
PPARA-Digitalis glycoside (−9.0 kcal·mol^{-1})

(e)



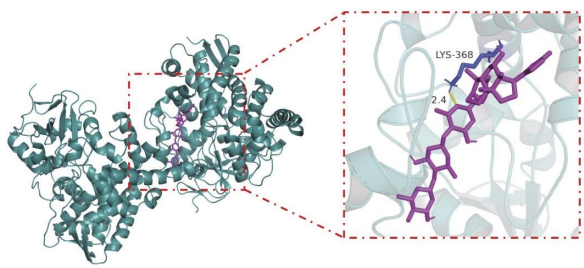
LDHA-Digitalis glycoside (−9.5 kcal·mol^{-1})

(f)



HIF1A-Digitalis glycoside (−9.1 kcal·mol^{-1})

(g)



EGFR-Digitalis glycoside (−9.5kcal·mol^{-1})

(h)

Figure 3: Bioinformatics analysis of key targets in the treatment of myocardial ischemia with *Polygonatum sibiricum*. Note: (a) Circular graph depicting the binding energy of each core target with active ingredient molecules. (b) Molecular docking of CYP19A1 and digitalis glycoside. (c) Molecular docking of MAPK1 and neoliquiritin. (d) Molecular docking of HIF-1α and neoliquiritin. (e) Molecular docking of PPARA and digitalis glycoside. (f) Molecular docking of LDHA and digitalis glycoside. (g) Molecular docking of HIF-1α and digitalis glycoside. (h) Molecular docking of EGFR and digitalis glycoside.

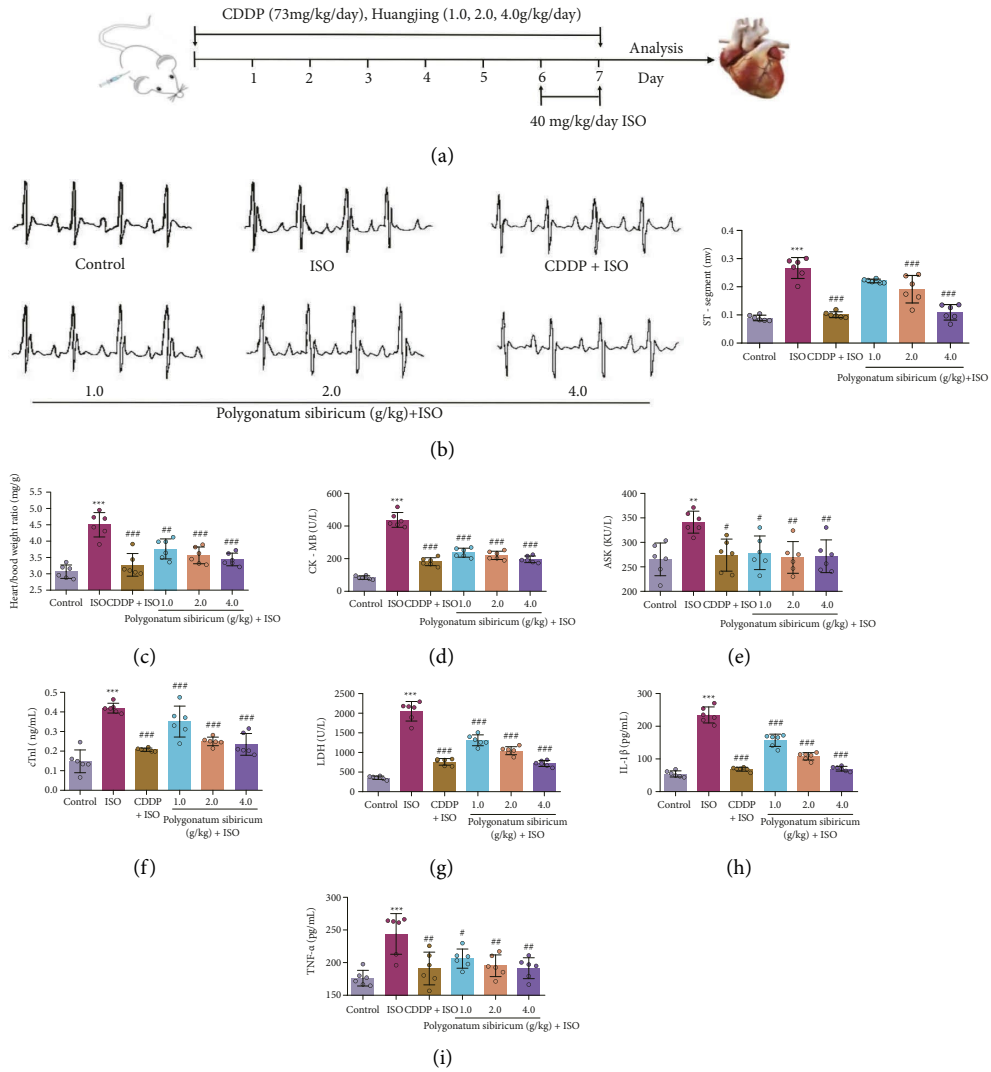


Figure 4: Effects of *Polygonatum sibiricum* on myocardial function and serum markers induced by ISO. Note: (a) Schematic representation of animal modeling experiments. (b) Analysis of rat electrocardiogram and changes in ST-segment elevation. (c) The ratio of heart weight to body weight in rats. (d) Levels of CK-MB in serum. (e) Levels of AST in serum. (f) Levels of cTnI in serum. (g) Levels of LDH in serum. (h) Levels of IL-1β in serum. (i) Levels of TNF-α in serum. Quantitative data represented as Mean ± SD, $n = 6$. $^{***}p < 0.001$ compared to the control group. $^{\#\#}p < 0.01$, $^{\#\#\#}p < 0.001$ compared to the ISO group.

The ECG is a highly sensitive indicator of ischemic myocardial changes. In rats, when the myocardium is damaged or necrotic, the ST segment of the ECG exhibits abnormal alterations. The deviation in the ST segment could be utilized as a quantitative measure of ischemia [34]. After the final administration, standard echocardiography was performed on the rats in each Group 24 h later at room temperature. Figure 4(b) demonstrates that rats induced with the ISO-induced MI model exhibited an ST-segment elevation compared to the Control group, as the ECG shows.

Conversely, the ECG of rats in the *Polygonatum sibiricum* treatment group and the positive drug group revealed a reduction of the ST segment compared to the ISO group. Cardiac hypertrophy in rats with a MI model was analyzed by comparing the heart-to-body weight ratio. The results revealed an increase in the heart-to-body weight ratio in the ISO group. In contrast, the *Polygonatum sibiricum* treatment group and the positive drug group showed a decrease in the heart-to-body weight ratio compared to the ISO group (Figure 4(c)). These results suggest that Codonopsis pilosula can potentially treat ISO-induced electrocardiographic abnormalities and inhibit ISO-induced cardiac hypertrophy dose-dependently.

Increased levels of cardiac biomarkers in the serum, including CK-MB, LDH, AST, and cTnI, are crucial indicators for diagnosing acute MI [35]. In normal circumstances, the serum levels of creatine kinase and inflammatory factors are typically low. Following MI or necrosis, cellular rupture occurs, causing the diffusion of intracellular enzymes into the bloodstream. This results in an elevation of myocardial enzyme levels in the blood [36].

To assess the impact of *Polygonatum sibiricum* on myocardial ischemic injury, we quantified the concentration of cardiac enzymes (CK-MB, AST, cTnI, and LDH) and inflammatory factors (IL-1β and TNF-α) in the serum. The experimental results revealed an increase in CK-MB, AST, cTnI, LDH, IL-1β, and TNF-α levels in the serum of rats in the ISO group compared to the control group. The *Polygonatum sibiricum* treatment group successfully reversed the expression levels of the factors above compared to the ISO group and exhibited a consistent trend similar to that of the positive drug group, as illustrated in Figures 4(d), 4(e), 4(f), 4(g), 4(h), 4(i).

This finding suggests that Rhizoma Polygonati could effectively suppress the abnormal elevation of serum biochemical indicators induced by ISO, demonstrating a dose-dependent response.

3.4. Protective Mechanisms of Polygonatum sibiricum in Ameliorating ISO-Induced Myocardial Damage and Oxidative Stress: Focus on Cellular and Mitochondrial Integrity. To enhance the understanding of the protective effect of *Polygonatum sibiricum* on myocardial tissue, we conducted HE staining and TTC staining on heart tissue from rats. The results revealed that the ISO group exhibited pathological damage to the myocardial tissue of rats, including extensive myocardial infarction, compared to the control group. In comparison with the ISO group, the *Polygonatum sibiricum* treatment group exhibited a relatively intact and clear structure of myocardial cells, as well as a reduction in the area of myocardial infarction and an improvement in myocardial damage (Figures 5(a) and 5(b)). Subsequently, the levels of oxidative stress in the heart tissue were evaluated using DHE staining and by measuring MDA, SOD, and GSH levels.

The results demonstrated that the fluorescence intensity of ISO-induced DHE (dihydroethidium) was higher in rat myocardial cells compared to the control group. Additionally, the expression of MDA was elevated, while the expression of SOD and GSH was reduced. Compared to the ISO group, the DHE treatment group with *Polygonatum sibiricum* exhibited a weaker fluorescence intensity, which counteracted the observed changes in these factors (Figures 5(c) and 5(d)). These findings suggest that *Polygonatum sibiricum* can decrease ISO-induced cardiac pathology and oxidative stress damage, and this effect appears to be dose-dependent.

Mitochondria are crucial organelles responsible for energy production and are extensively distributed within myocardial cells. Oxidative stress in the heart makes mitochondria vulnerable to attack by ROS, resulting in mitochondrial dysfunction and impacting the onset and progression of myocardial infarction [24].

To verify the protective effect of *Polygonatum sibiricum* on mitochondria, transmission electron microscopy was employed to examine the ultrastructure of cardiac myocyte mitochondria (Figure 5(e)). The findings suggest that the ISO group demonstrated mitochondrial swelling, ridge rupture, and dissolution into vesicles compared to the control group. Compared to the ISO group, the *Polygonatum sibiricum* treatment group exhibited lower ultrastructural damage in the myocardial mitochondria. Furthermore, we assessed the activity of mitochondrial enzymes in the cardiac tissue. The ISO group exhibited lower SDH and MDH activity levels than the control group. Compared to the ISO group, SDH and MDH activities were increased in the *Polygonatum sibiricum* treatment group (Figure 5(f)). This result suggests that *Polygonatum sibiricum* may protect the mitochondrial structure and maintain its function in myocardial cells, with a relationship that depends on the dosage.

These findings suggest that *Polygonatum sibiricum* can potentially protect the mitochondrial structure of cardiomyocytes and preserve their function. This protection may inhibit the pathological damage and oxidative stress induced by ISO.

3.5. Dose-Dependent Inhibition of Cardiomyocyte Apoptosis by Polygonatum sibiricum Through Regulation of HIF-1α and Associated Proteins. In addition, we utilized TUNEL staining to identify apoptosis of myocardial cells in cardiac tissue. The results demonstrated an increase in the apoptosis index of rat myocardial cells in the ISO group compared to the control group. The *Polygonatum sibiricum* treatment group demonstrated a decrease in the myocardial cell apoptosis index (Figure 6(a)) compared to the ISO group. We conducted a Western blot analysis to assess apoptosis-related proteins Bax, C-caspase-3, and Bcl-2 expression levels in cardiac tissue. The results are shown in Figures 6(b) and 6(c).

The results demonstrated that the ISO group exhibited an increase in the expression of Bax and C-caspase-3 proteins, accompanied by a noteworthy decrease in the expression of Bcl-2 protein compared to the control group. Compared to the ISO group, the group treated with *Polygonatum sibiricum* exhibited a substantially reduced expression of Bax and C-caspase-3 proteins, whereas the expression of Bcl-2 protein increased. These results indicate that Rhizoma Polygonati Odorati can inhibit apoptosis in ISO-induced myocardial cells, and its effect depends on the dosage. Previous literature reports have demonstrated that HIF-1α regulates myocardial cell apoptosis through multiple pathways. For instance, the overexpression of HIF-1α could enhance HO-1 expression and suppress oxidative stress-induced damage in myocardial cells, ultimately mitigating myocardial cell apoptosis [27, 30].

Analyzing the KEGG pathway using network pharmacology, we discovered that *Polygonatum sibiricum* can potentially treat MI by regulating the HIF-1α signaling pathway. To determine the specific role of HIF-1α in treating MI with Rhizoma Polygonati, we performed Western blot analysis to measure the expression levels of both HIF-1α and HO-1 in cardiac tissues. The results demonstrated increased protein expressions of HIF-1α and HO-1 in the ISO group compared to the control group. In the *Polygonatum sibiricum* treatment group, compared to the ISO group, the expressions of HIF-1α and HO-1 proteins were also

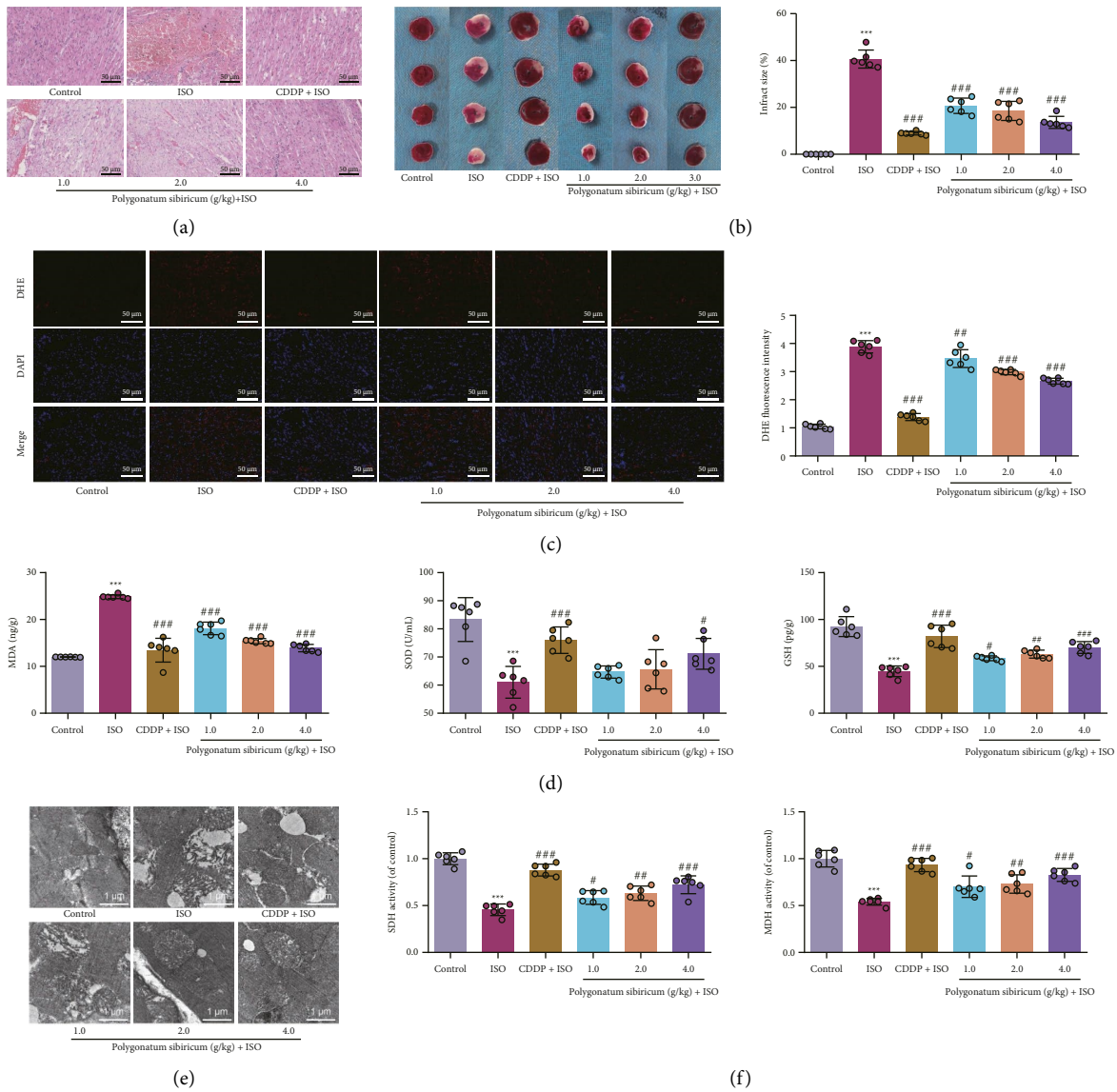


FIGURE 5: Protective effect of *Polygonatum sibiricum* on myocardial ischemia induced by ISO in rats. Note: (a) H&E staining of rat heart tissue (scale bar = 50 μm). (b) TTC staining of heart tissue and percentage of infarct size. (c) DHE staining of heart tissue (scale bar = 50 μm) and DHE fluorescence intensity. (d) MDA, SOD, and GSH activity in heart tissue. (e) Transmission electron microscopy of cardiac mitochondria (scale bar: 1 μm). (f) SDH and MDH activity in heart tissue. Quantitative data represented as Mean ± SD, $n = 6$. $^{***}p < 0.001$ compared to the control group. $^{\#}p < 0.05$, $^{\#\#}p < 0.01$, $^{\#\#\#}p < 0.001$ compared to the ISO group.

increased (Figure 6(d)). It suggests that *Polygonatum sibiricum* can enhance the expression of HIF-1α and HO-1, which positively correlates with dosage.

In summary, the results above demonstrate the inhibitory effects of *Polygonatum sibiricum* on cardiomyocyte apoptosis. The mechanism underlying this effect may be associated with regulating the HIF-1α pathway.

3.6. In Vitro Validation of Polygonatum sibiricum's Protective Effects on MI: Mitochondrial Integrity, Cell Viability, and HIF-1α Pathway Regulation. Additional evidence supporting the protective effects of Rhizoma Polygonati on mitochondrial function and myocardial ischemic injury has been acquired through in vitro cell experiments. In our in vivo animal experiments, we discovered that Rhizoma Polygonati extract protects against MI. This effect is likely attributed to the extract's ability to safeguard mitochondrial energy metabolism through the HIF-1α pathway. To elucidate the protective effect and mechanism of *Polygonatum sibiricum* against MI, we utilized ISO-induced H9c2 cells as an in vitro cell model. Before conducting cell experiments, we predetermined the concentration of *Polygonatum sibiricum* to be 2.0 mg/mL (Figure 7(a)).

The cell viability assay results demonstrated a decrease in cell viability in the ISO group compared to the control group. Furthermore, the *Polygonatum sibiricum* + ISO group exhibited increased cell viability compared to the ISO group (Figure 7(b)). The analysis of LDH release indicated that the ISO group had a higher LDH release rate than the control

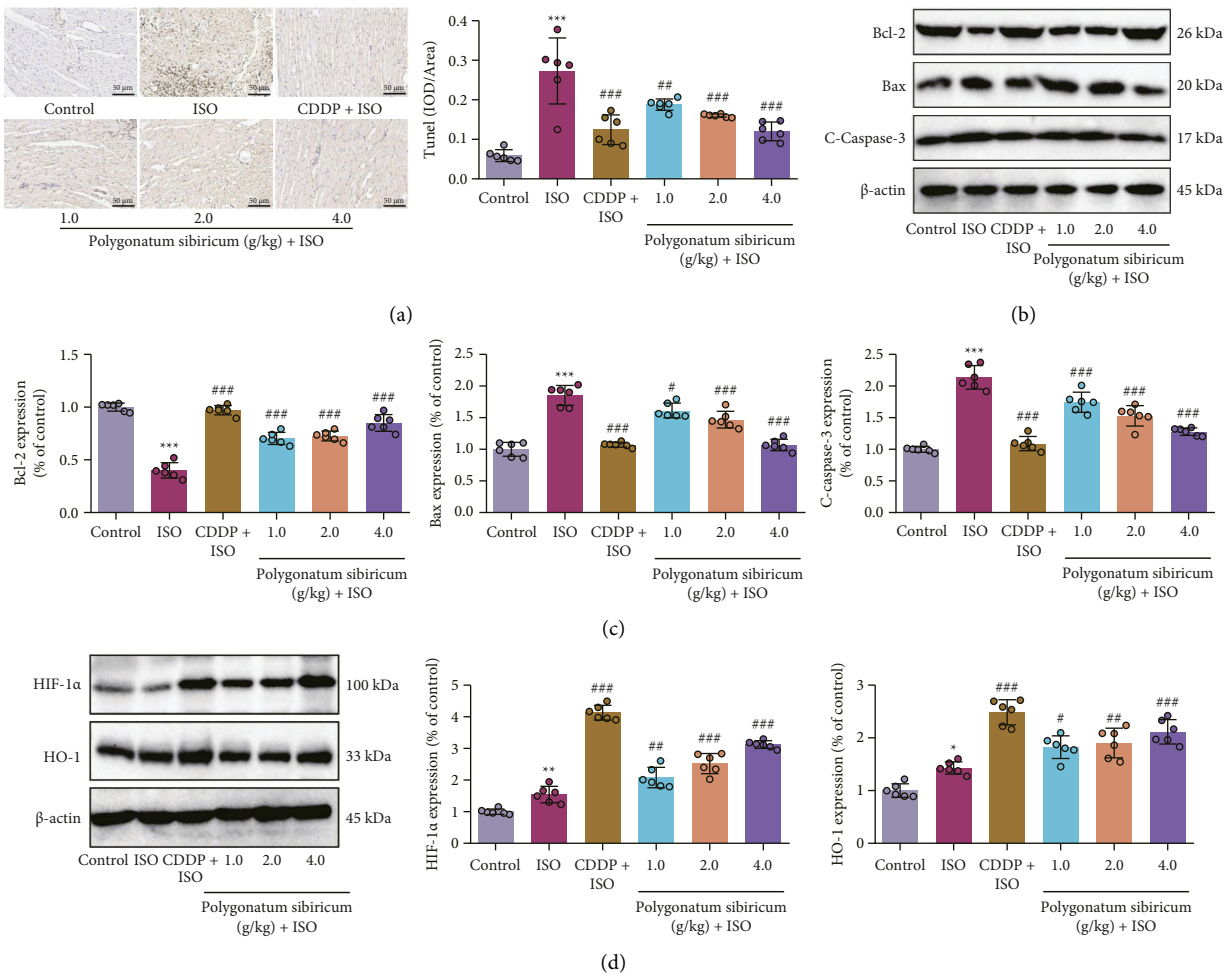


Figure 6: Effects of *Polygonatum sibiricum* on apoptosis in ISO-induced rat myocardium. Note: (a) TUNEL staining of heart tissue (scale bar = 50 μm) and apoptosis rate of myocardial cells. (b) Protein expression of Bcl-2, Bax, C-caspase-3, and β-actin in heart tissue. (c) Expression levels of Bcl-2, Bax, and C-caspase-3 in heart tissue. (d) Protein expression of HIF-1α and HO-1 in heart tissue. Quantitative data represented as Mean ± SD, $n = 6$. $^{***}p < 0.001$ compared to the control group. $^{\#}p < 0.05$, $^{\#\#}p < 0.01$, $^{\#\#\#}p < 0.001$ compared to the ISO group.

group. Furthermore, the *Polygonatum sibiricum* + ISO group showed a decrease in LDH release rate compared to the ISO group (Figure 7(c)). Subsequently, we analyzed the alterations in mitochondrial membrane potential, calcium (Ca^{2+}) levels, and ROS levels in H9c2 cells. It was achieved by corresponding staining techniques using Rh123, Fluo-3 AM, DCFH-DA, and DHE.

The results demonstrated an increase in the fluorescence intensity of Fluo-3 AM, DCFH-DA, and DHE in the ISO group compared to the control group, whereas the fluorescence intensity of Rh123 notably decreased. Additionally, the *Polygonatum sibiricum* + ISO group exhibited a reversal of these changes compared to the ISO group (Figures 7(d), 7(e), 7(f), 7(g)). These findings indicate that *Polygonatum sibiricum* can potentially prevent Ca^{2+} overload and preserve mitochondrial structure by reducing ROS levels, thus preventing mitochondrial dysfunction in cardiomyocytes.

Furthermore, we utilized the V-FITC/PI staining method to examine apoptosis in H9c2 cells. The results revealed a higher rate of cell apoptosis in the ISO group compared to the control group. Conversely, the *Polygonatum sibiricum* + ISO group exhibited a reduction in cell apoptosis compared to the ISO group (Figure 7(h)). The protein imprinting method determined the expression levels of Bax, C-caspase-3, and Bcl-2 in H9c2 cells. Compared to the control group, the ISO group demonstrated an increase in the expression of Bax and C-caspase-3 proteins, whereas the expression of Bcl-2 was decreased. The *Polygonatum sibiricum* + ISO group reverses the expression levels of these proteins in comparison with the ISO group (Figure 7(i)).

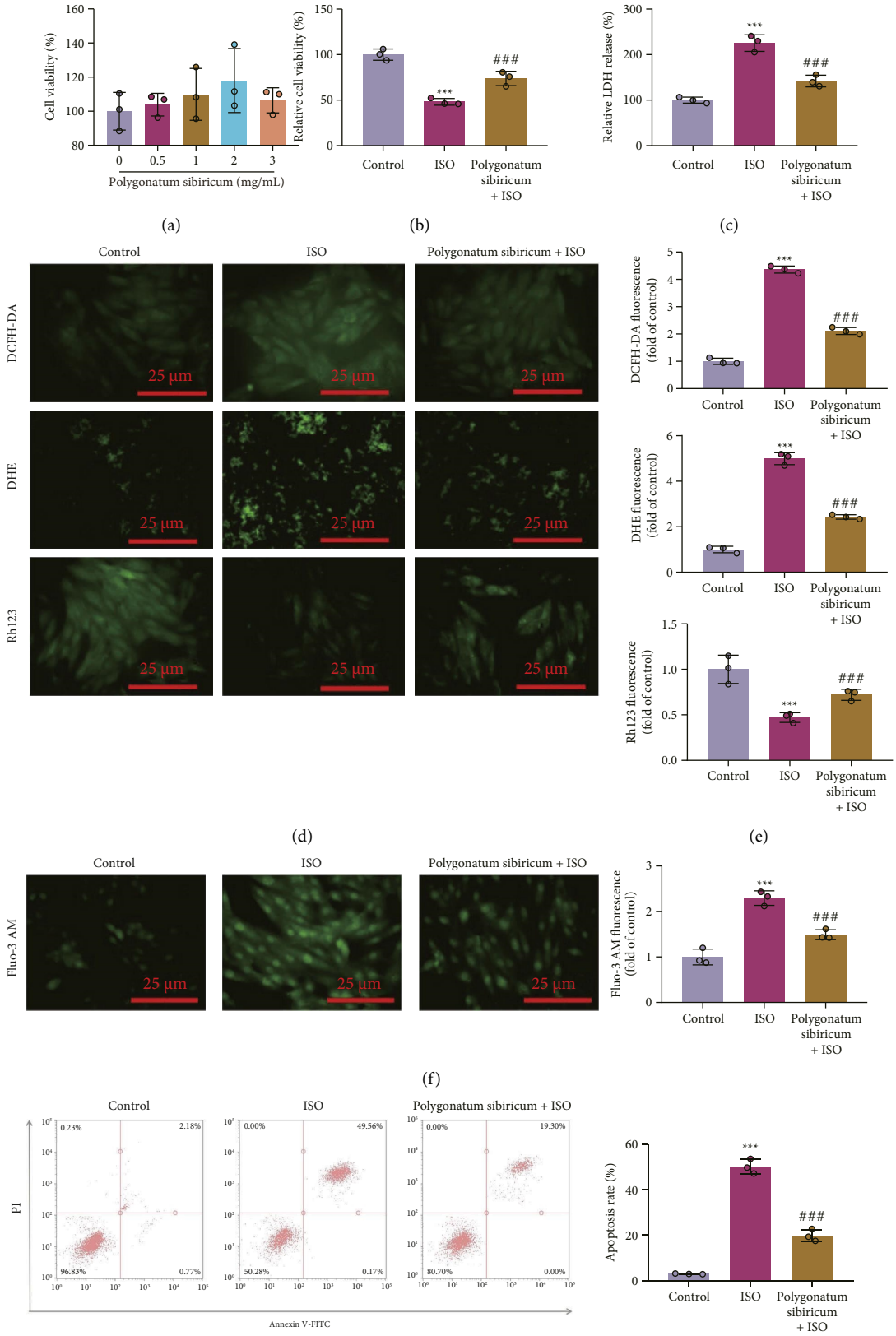


FIGURE 7: Continued.

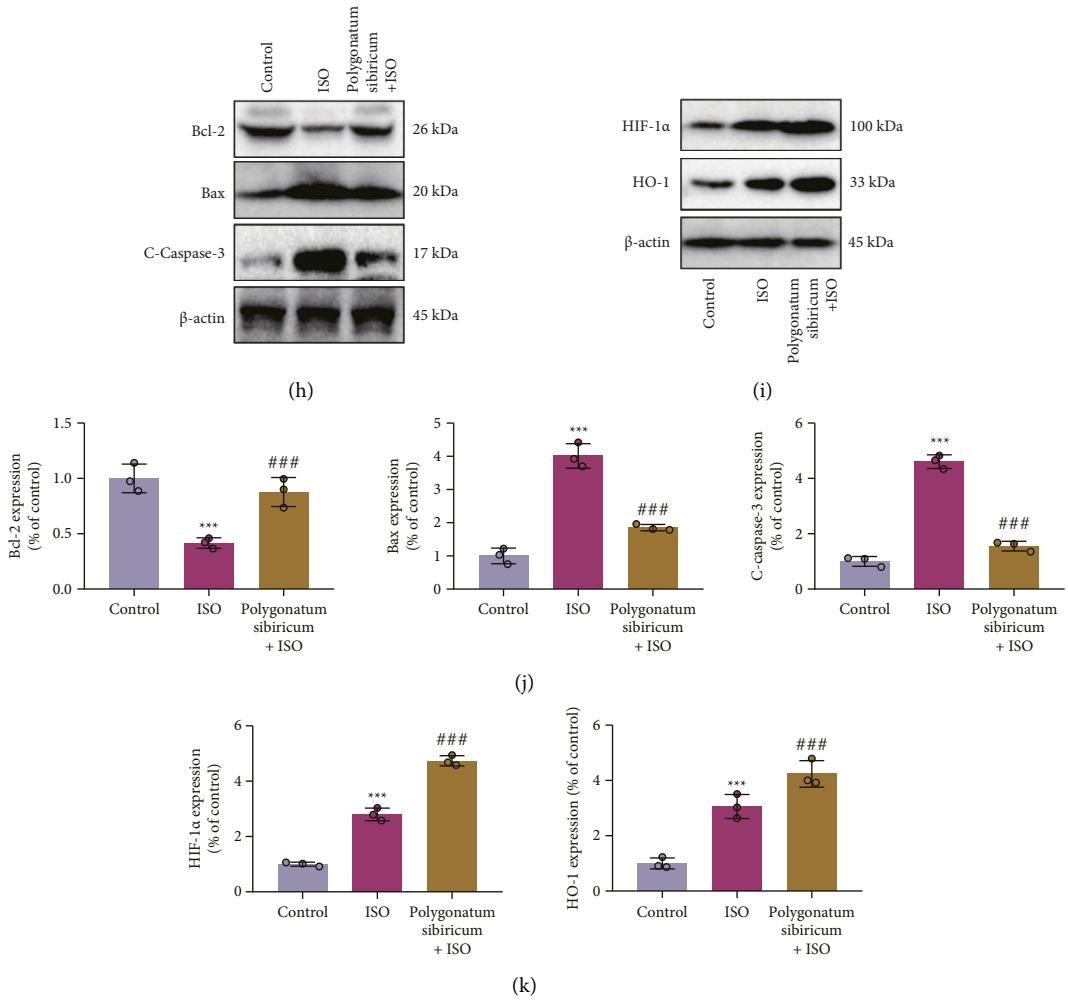


Figure 7: Protective effect of *Polygonatum sibiricum* on ISO-induced myocardial cell injury in vitro. Note: (a) Effects of different concentrations of *Polygonatum sibiricum* on H9c2 myocardial cell viability. (b) MTT assay of cell viability. (c) Evaluation of cell damage by LDH release assay in H9c2 cells. (d) DCFH-DA, DHE, and Rh123 staining of H9c2 cells (scale bar = 25 μm). (e) Fluorescence intensity of DCFH-DA, DHE, and Rh123 in H9c2 cells. (f) Fluo-3 AM staining and fluorescence intensity in H9c2 cells (scale bar = 50 μm). (g) Membrane-associated protein-V/PI staining and apoptotic rate in H9c2 cells. (h) Expression levels of Bcl-2, Bax, and C-caspase-3 in H9c2 cells; (i) Expression levels of HIF-1α and HO-1 in H9c2 cells. (j) Statistical analysis of expression levels of Bcl-2, Bax, and C-caspase-3 in H9c2 cells. (k) Statistical analysis of expression levels of HIF-1α and HO-1 in H9c2 cells. Quantitative data represented as Mean ± SD, $n = 6$. $^{***}p < 0.001$ compared to the control group. $^{###}p < 0.001$ compared to the ISO group. Cell experiments were independently repeated three times.

These findings indicate that *Polygonatum sibiricum* can inhibit ISO-induced myocardial cell apoptosis.

Moreover, the protein imprinting method was used to further detect the expression of HIF-1α and HO-1 in H9c2 cells. The results indicated that the ISO group exhibited higher expression levels of HIF-1α and HO-1 proteins than the control group. Compared to the ISO group, the *Polygonatum sibiricum* + ISO group demonstrated a greater increase in the expression of HIF-1α and HO-1 proteins (Figures 7(j) and 7(k)).

Consistent with the findings of prior in vitro experiments, these experimental results further validate the inhibitory effect of *Polygonatum sibiricum* on myocardial cell apoptosis. The mechanism of action may be linked to the regulatory effect of the HIF-1α pathway.

3.7. Knockdown of HIF-1α Validates Its Crucial Role in Polygonatum sibiricum-Mediated Protection Against Myocardial Ischemic Injury. To further validate the regulatory role of HIF-1α, we transfected si-HIF-1α to suppress the expression of HIF-1α in H9c2 cells (Figure 8(a)). Subsequently, we examined the protective effect of *Polygonatum sibiricum* on cardiac cells. The results of the cell viability and apoptosis experiments indicate that, in comparison with the *Polygonatum sibiricum* + ISO + si-NC group, the *Polygonatum sibiricum* + ISO + si-HIF-1α#1 group demonstrated a substantial decrease in the viability of H9c2 cells and a notable increase in apoptosis (Figures 8(b) and 8(c)).

The Western blot results demonstrated a decrease in the expression of Bcl-2 compared to the *Polygonatum sibiricum* + ISO + si-NC group, while the expression of Bax

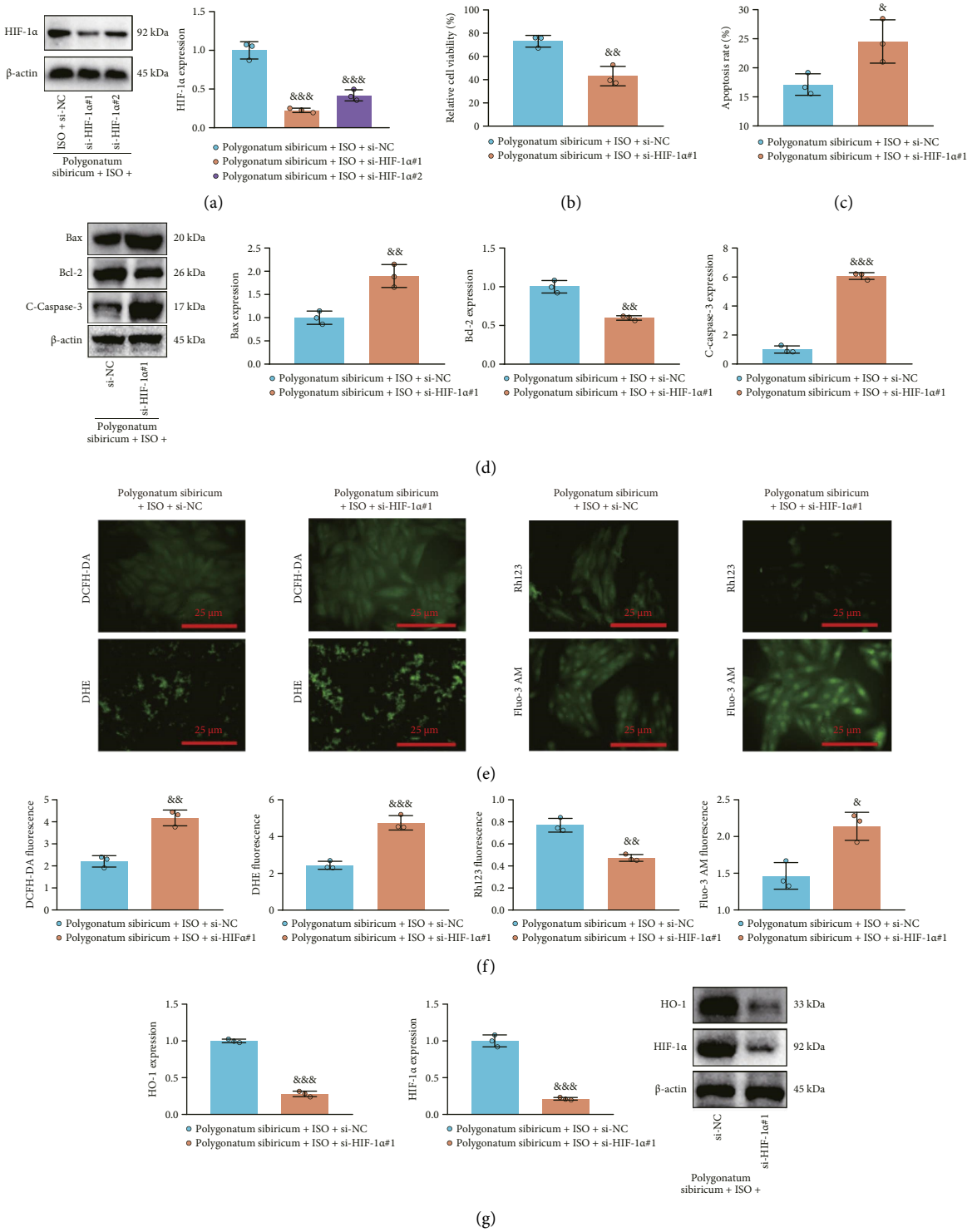


Figure 8: Effects of si-HIF-1α transfection on H9c2 cardiomyocytes. Note: (a) Transfection efficiency of si-HIF-1α#1 and si-HIF-1α#2. (b) Proliferation of H9c2 cardiomyocytes after si-HIF-1α transfection. (c) Apoptosis of H9c2 cardiomyocytes after si-HIF-1α transfection. (d) Western blot analysis and expression of Bcl-2, Bax, and C-caspase-3 proteins in si-HIF-1α-transfected H9c2 cardiomyocytes. (e) Staining of si-HIF-1α-transfected H9c2 cells with DCFH-DA, DHE, Rh123, and Fluo-3 AM (scale bar = 25 μm). (f) Fluorescence intensity of DCFH-DA, DHE, Rh123, and Fluo-3 AM in si-HIF-1α-transfected H9c2 cells. (g) Western blot analysis and expression of HIF-1α and HO-1 proteins in si-HIF-1α-transfected H9c2 cardiomyocytes. Quantitative data are presented as Mean ± SD, $n = 6$. Statistical comparisons were made against the *Polygonatum sibiricum* + ISO + si-NC group: $^{\&}p < 0.05$, $^{\&\&}p < 0.01$, $^{\&\&\&}p < 0.001$. Cell experiments were independently repeated 3 times.

and C-caspase-3 was increased in the *Polygonatum sibiricum* + ISO + si-HIF-1α#1 group (Figure 8(d)).

Subsequently, we analyzed the levels of Ca^{2+} using Fluo-3 AM staining, the changes in mitochondrial membrane potential using Rh123 staining, and the levels of ROS using DCFH-DA and DHE staining in H9c2 cells transfected with si-HIF-1α. The results revealed that the fluorescence intensity of Fluo-3 AM, DCFH-DA, and DHE increased in the *Polygonatum sibiricum* + ISO + si-HIF-1α#1 group compared to the *Polygonatum sibiricum* + ISO + si-NC group. However, the fluorescence intensity of Rh123 was reduced, as observed in Figures 8(e) and 8(f). These findings suggest that downregulating HIF-1α expression enhances the generation of ROS, augments the oxidative stress response, and heightens mitochondria's vulnerability to ROS attacks. Simultaneously, the rise in intracellular Ca^{2+} induces mitochondrial dysfunction.

Furthermore, we assessed the expression of HIF-1α and HO-1 in H9c2 cells transfected with si-HIF-1α through a protein imprinting assay. The results indicated a reduction in the expression levels of HIF-1α and HO-1 in the *Polygonatum sibiricum* + ISO + si-HIF-1α#1 group (Figure 8(g)) compared to the *Polygonatum sibiricum* + ISO + si-NC group.

These findings suggest that *Polygonatum sibiricum* can activate the HIF-1α pathway, safeguard mitochondrial function, and enhance myocardial ischemic injury caused by ISO.

3.8. Metabolomics Insights Into Polygonatum sibiricum's Regulation of the Tricarboxylic Acid Cycle and Energy Metabolism in MI. To investigate the metabolic mechanism of *Polygonatum sibiricum* in treating MI, we conducted a metabolomics study on rat plasma samples using UHPLC-Q-TOF/MS technology.

PCA and OPLS-DA results demonstrate clear differentiation between the ISO group (blue) and the control group (green) in both positive and negative ion modes. Furthermore, the positive drug group (CDDH, red) and high-dose *Polygonatum sibiricum* group (HJ, yellow) are also significantly separate from the ISO group (Figures 9(a), 9(b), 9(c), 9(d), 9(e), 9(f), 9(g)). These findings suggest that ISO has a notable impact on the metabolites in rats, and *Polygonatum sibiricum* has the potential to alleviate this effect.

Furthermore, we employed one-way ANOVA to identify potential biomarkers associated with the antimyocardial ischemic mechanism of *Polygonatum sibiricum* (Figure 9(h)). In total, 39 potential biomarkers were screened, as shown in Table S4. Compared to the control group, the levels of important metabolites associated with the tricarboxylic acid cycle, including alpha-ketoglutarate, fumarate, and succinylacetone, were diminished in the rat plasma of the ISO group. Conversely, the levels of citrate and malate were increased. These observations suggest that the MI model disrupts the steady state of the tricarboxylic acid cycle, leading to interference in the energy supply. Compared to the ISO group, *Polygonatum sibiricum* effectively restored the levels of the aforementioned potential biomarkers. It indicates that *Polygonatum sibiricum* potentially maintains tricarboxylic acid cycle homeostasis by intervening in these compounds, thereby ensuring energy supply during myocardial ischemic conditions.

Additionally, we conducted a heatmap analysis (Figure 9(i)) to examine these potential biomarkers. The graph clearly shows differences in plasma levels among them, thus demonstrating their remarkable discriminatory ability. We analyzed the metabolic pathways closely associated with these 39 differential markers in detail (Figure 9(j)). Our findings reveal the critical involvement of the tricarboxylic acid cycle and amino acid metabolism pathways, specifically relating to energy metabolism (including glutamine, glutamate, alanine, and aspartate), in regulating MI.

The heart is the organ responsible for powering the circulatory system, and its continuous functioning necessitates adequate energy support. MI directly damages energy metabolism [37]. The tricarboxylic acid cycle is an essential process in energy metabolism that takes place in the mitochondrial matrix. During the tricarboxylic acid cycle, glucose is subjected to glycolysis, resulting in the production of pyruvate. Subsequently, pyruvate undergoes conversion to acetyl-CoA, which then enters the cycle. The active hydrogen produced by this cycle is ultimately converted into a quantity of adenosine triphosphate (ATP) through oxidative phosphorylation. ATP is the primary energy source for aerobic respiration [38]. *Polygonatum sibiricum* can potentially enhance myocardial ischemic injury by modulating energy metabolism and preserving mitochondrial functional homeostasis via the tricarboxylic acid cycle.

4. Discussion

This study comprehensively investigated the interaction between 11 main active ingredients of the traditional Chinese medicine *Polygonatum sibiricum* and 23 core target proteins, including HIF-1α (Figure 10). This comprehensive analysis unveils the diverse mechanisms by which *Polygonatum sibiricum* acts. It offers a novel theoretical foundation for the management of myocardial ischemic injury and has the potential to advance both research and treatment in the cardiovascular disease field [39].

This study extensively investigates the protective effect of *Polygonatum sibiricum* on MI, as well as its underlying mechanisms [6]. Experimental data showed that *Polygonatum sibiricum* can effectively reverse the ISO-induced abnormal changes in ECG and serum biomarkers by activating the HIF-1α pathway, thereby demonstrating its strong cardioprotective effect [6]. Furthermore, *Polygonatum sibiricum* has the ability to substantially decrease the size of myocardial infarction, as well as enhance the pathological condition of cardiac tissue. These findings further underscore its therapeutic effectiveness in the treatment of MI [6]. This series of discoveries not only supports the efficacy of *Polygonatum sibiricum* in treating MI but also offers robust evidence for its potential clinical applications [40].

This study highlights the significance of the HIF-1α pathway in the treatment of MI using *Polygonatum sibiricum* [41]. The research findings suggest that HIF-1α plays a vital role in the treatment of *Polygonatum sibiricum*. In this study,

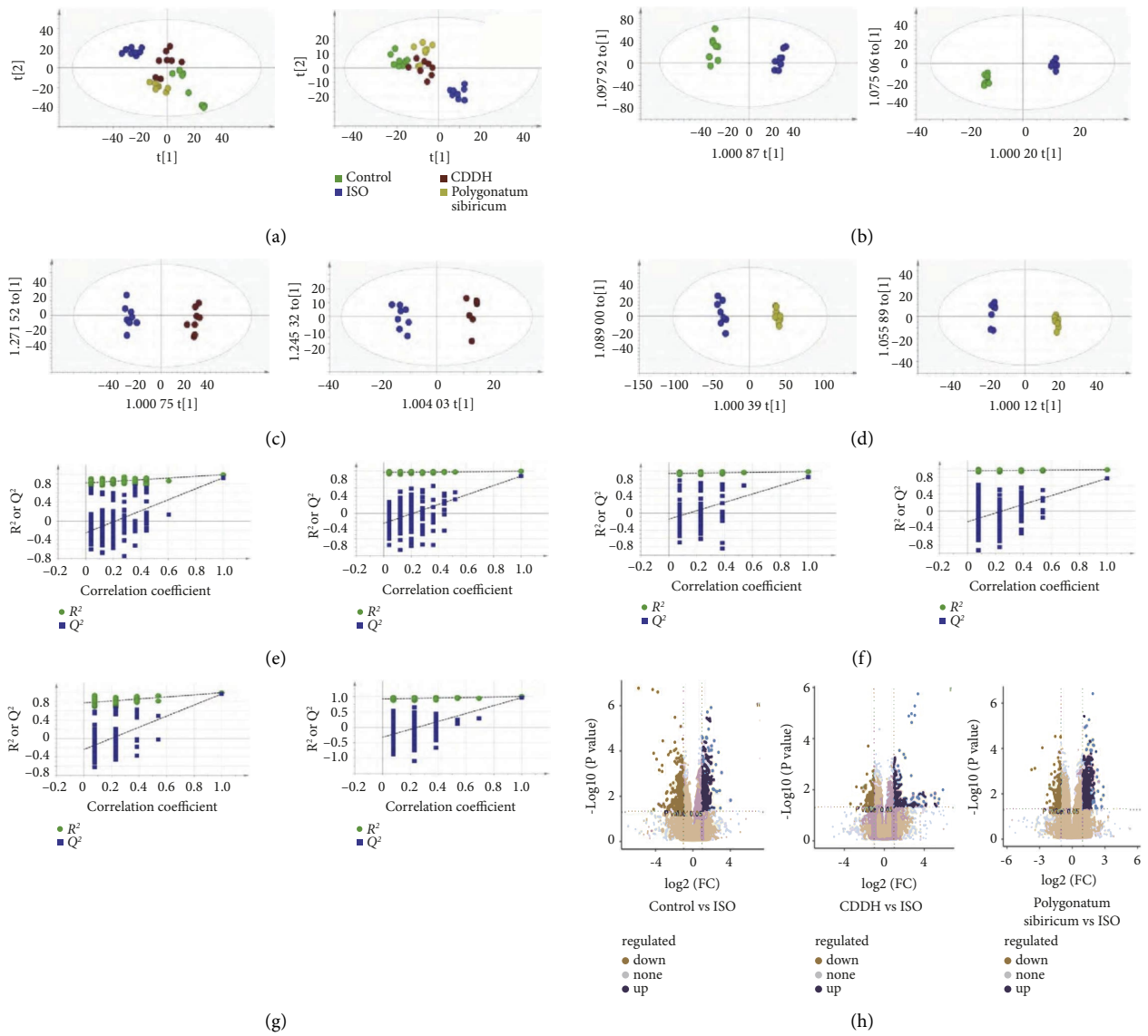
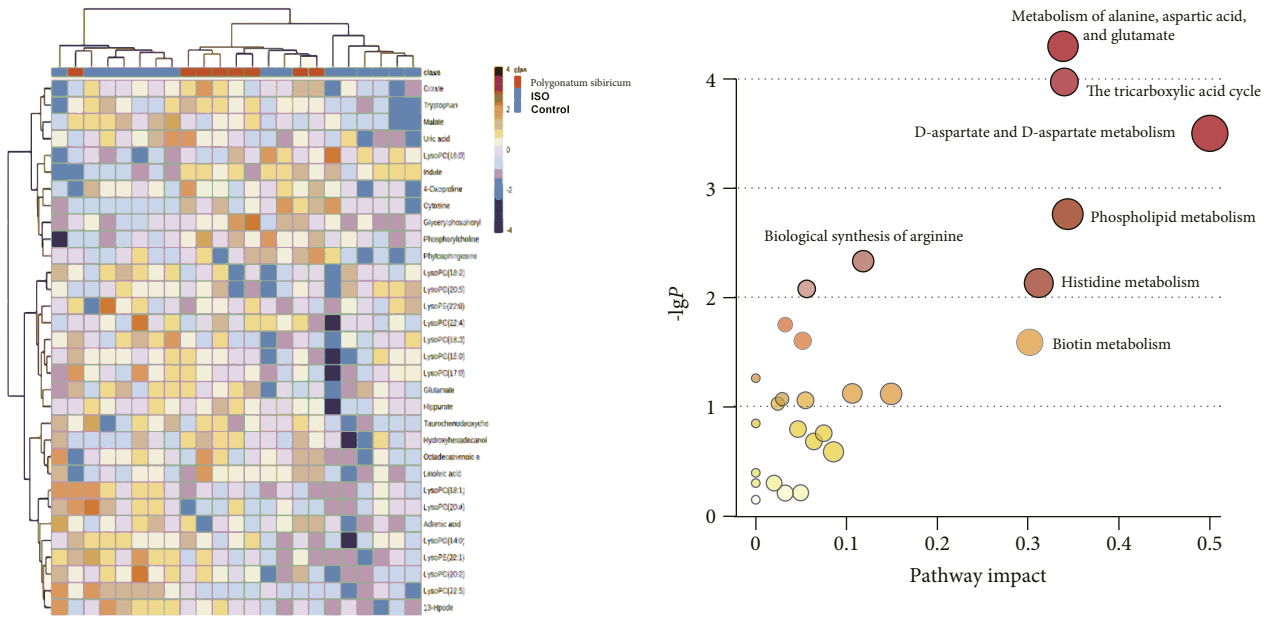


Figure 9: Continued.



(i) (j)

Figure 9: Metabolomic analysis of myocardial ischemia induced by ISO in rats. Note: (a) PCA score plot of serum samples from the four groups of rat in positive and negative ion modes ($n = 6$). (b) OPLS-DA score plot of the ISO group compared to the control group in both positive and negative ion modes. (c) OPLS-DA score plot of the positive drug group compared to the ISO group in both positive and negative ion modes. (d) OPLS-DA score plot of high-dose *Polygonatum sibiricum* group (*Polygonatum sibiricum*) compared to ISO group in both positive and negative ion modes. (e) OPLS-DA permutation validation results for the ISO group compared to the control group in both positive and negative ion modes. (f) OPLS-DA permutation validation results for the positive drug group compared to the ISO group in both positive and negative ion modes. (g) OPLS-DA permutation validation results for the high-dose *Polygonatum sibiricum* group (*Polygonatum sibiricum*) compared to the ISO group in both positive and negative ion modes. (h) Volcano plot of differential metabolites based on FC values and p values. (i) Heatmap of differential metabolites. (j) Bubble plot of KEGG enrichment analysis of differential metabolites.

we also experimentally measured oxidative stress-related indicators, such as SOD, MDA, GSH, and ROS levels, to confirm that *Polygonatum sibiricum* can regulate the oxidative stress pathway and thereby alleviate myocardial ischemic symptoms (Figures 5(c), 5(d), 8(e), 8(f)). Therefore, it can be preliminarily concluded that the HIF-1α pathway and oxidative stress pathway potentially interact in the regulation of MI. Additionally, studies have shown [42] that the flavonoid compound *Latifolin* can improve myocardial inflammation via the HIF-1α/NF-κB/IL-6 signaling pathway, thereby preventing myocardial infarction. Based on the conclusions of this study, we propose that the HIF-1α pathway may also interact with inflammation-related signaling pathways in the regulation of myocardial diseases. Moreover, the suppression of its expression substantially diminishes the therapeutic efficacy of *Polygonatum sibiricum* [41]. Furthermore, the study conducted an additional investigation on the correlation between *Polygonatum sibiricum*, myocardial energy metabolism, and mitochondrial function. The findings elucidate the mechanisms by which *Polygonatum sibiricum* enhances myocardial ischemic injury recovery through the regulation of these BPs [21]. This study elucidates the pivotal role of the HIF-1α pathway in the cardioprotective effects of *Polygonatum sibiricum* against MI [43]. Our study revealed that the activation of the HIF-1α pathway by *Polygonatum sibiricum* has a significant improvement in MI [41]. However, the therapeutic effect of *Polygonatum sibiricum* is significantly limited when the expression of HIF-1α is suppressed, thereby reaffirming the crucial role of HIF-1α [41]. Further research has demonstrated the effectiveness of *Polygonatum sibiricum* in combating MI through the regulation of energy metabolism and mitochondrial function. These findings form a solid foundation for future research and applications of *Polygonatum sibiricum* [21].

We confirmed that *Polygonatum sibiricum* has the ability to inhibit oxidative stress damage and myocardial cell apoptosis induced by ISO [6]. This finding is in line with prior research on the correlation between oxidative stress and cell apoptosis [44]. The potential of *Polygonatum sibiricum* can be attributed to the combined effects of its numerous active ingredients, which lay the groundwork for further medicinal development of the herb [45]. This study provides the initial confirmation that *Polygonatum sibiricum* can protect mitochondrial function through the activation of the HIF-1α pathway [46]. Mitochondria, often referred to as the "powerhouse" of cells, are known to have a crucial role in MI as their function becomes impaired [47]. The protective effect of *Polygonatum sibiricum* on mitochondria further demonstrates its significance in the treatment of MI [48]. We employed UPLC-Q/TOF-MS technology to carry out metabolomics analysis, which provides a significant contribution to the investigation of the mechanism of *Polygonatum sibiricum* [49]. Using metabolomics, we have

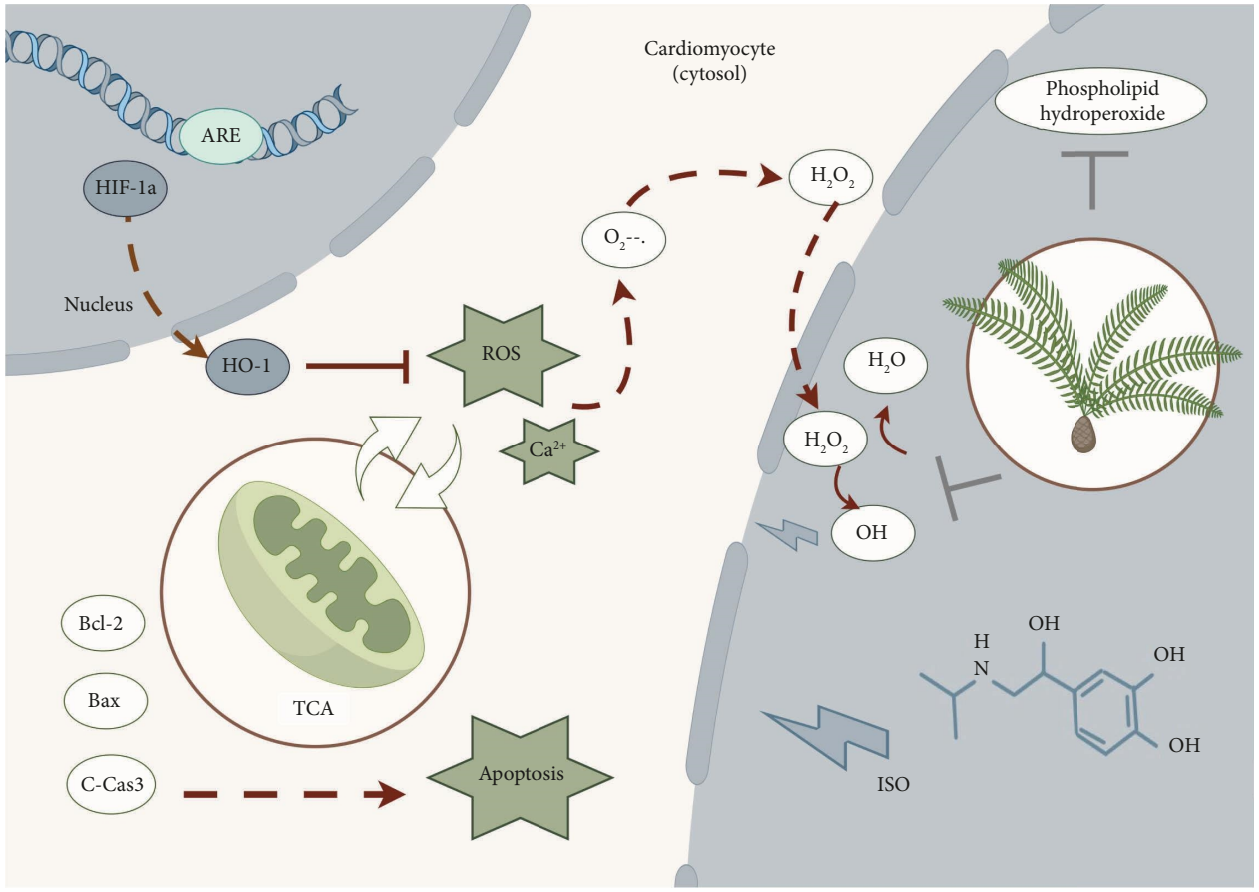


FIGURE 10: Molecular mechanism diagram illustrating *Polygonatum sibiricum* activation of the HIF-1α pathway to improve myocardial ischemic injury.

uncovered the correlation between *Polygonatum sibiricum* and the management of MI, as well as its impact on energy metabolism through the tricarboxylic acid cycle. These findings contribute to a better comprehension of its mechanism of action [50].

Although this study identified the HIF-1α pathway as a key target for *Polygonatum sibiricum* in the treatment of MI, there exist numerous intersecting and complex signaling pathways in biological systems, and the HIF-1α pathway may only be one of them. Considering the importance of the HIF-1α pathway, future studies could explore combining *Polygonatum sibiricum* with drugs targeting other related pathways to achieve enhanced therapeutic effects. Further investigation of other active components in *Polygonatum sibiricum* is also warranted. While this study identified 11 major active components, *Polygonatum sibiricum* may contain other undiscovered effective ingredients that merit further research.

5. Conclusion

In this study, the potential therapeutic effects of *Polygonatum sibiricum* on MI were preliminarily validated using a rat MI model. However, the model has limitations, such as differences in pathophysiology between rats and humans. Future research will adopt animal models that more closely mimic human pathology and incorporate multiple models to minimize bias. Gene-editing technology will be employed to construct disease models, and their accuracy will be verified by comparing gene expression and proteomics data with human samples. Additionally, human cell-based microphysiological systems will be used to simulate organ function, and pharmacokinetic and pharmacodynamic models will be developed to design precise dosing regimens.

To address potential biases in network pharmacology predictions, future studies will optimize algorithms—such as machine learning—and integrate multisource data to improve prediction accuracy. These predictions will also be validated using independent clinical datasets. Moreover, transparency and reproducibility will be ensured by providing detailed reports of data sources, analytical methods, and results. In summary, this study offers novel perspectives and approaches for the treatment of MI with *Polygonatum sibiricum*, providing valuable insights for future research and clinical applications. However, the signaling pathways and molecular mechanisms explored in this study do not represent the entirety of MI's underlying mechanisms. Other unknown BPs may also be involved, and these warrant further investigation.

Data Availability Statement

The datasets generated and/or analyzed during the current study are available from the corresponding author upon reasonable request.

Ethics Statement

The Institutional Animal Ethics Committee of Yongkang First People's Hospital Affiliated to Hangzhou Medical College (No. SCXK 2020-017) has approved the experimental protocol and animal use plan.

Consent

The authors have nothing to report.

Conflicts of Interest

The authors declare no conflicts of interest.

Author Contributions

Zhenzhong Zhu conceived and designed the research. Junzhi Pan performed experiments. Bin Jiang interpreted results of experiments. Yuanlong Zhang analyzed the data. Yanxia Lv prepared figures. Yifan Pan drafted the paper. Yunxiang Wang and Weijun Lv edited and revised the manuscript. All authors read and approved the final version of manuscript. Zhenzhong Zhu and Junzhi Pan are co-first authors.

Funding

This study was supported by the Hospital Pharmacy Special Research Project of Zhejiang Pharmaceutical Society (2022ZYY50), General Science and Technology Project of the Zhejiang Provincial Department of Education (Y202249201), and Foundation of TCM Science and Technology Project of Zhejiang Province (2023ZF185). and Jinhua City Science and Technology Project (No. 2024-4-309).

Acknowledgments

The authors have nothing to report.

Supporting Information

Additional supporting information can be found online in the Supporting Information section. *(Supporting Information)*

Table S1: Summary table of *Polygonatum sibiricum* active compounds.

Table S2: The binding energy of the main active ingredients and core targets of *Polygonatum sibiricum*.

Table S3: Various chemical components identified from *Polygonatum sibiricum*.

Table S4: Potential biomarkers related to *Polygonatum sibiricum*'s antimyocardial ischemia effect.

References

[1] Z. Li, Y. Ding, Y. Peng, et al., "Effects of IL-38 on Macrophages and Myocardial Ischemic Injury," *Frontiers in Immunology* 13 (2022): 894002, https://doi.org/10.3389/fimmu.2022.894002.

[2] M. Cohen and G. Visveswaran, "Defining and Managing Patients With Non-ST-Elevation Myocardial Infarction: Sorting Through Type 1 vs Other Types," *Clinical Cardiology* 43, no. 3 (2020): 242–250, https://doi.org/10.1002/clc.23308.

[3] A. Deichl, R. Wachter, and F. Edelmann, "Comorbidities in Heart Failure With Preserved Ejection Fraction," *Herz* 47, no. 4 (2022): 301–307, https://doi.org/10.1007/s00059-022-05123-9.

[4] S. K. Law, Y. Wang, X. Lu, et al., "Chinese Medicinal Herbs as Potential Prodrugs for Obesity," *Frontiers in Pharmacology* 13 (2022): 1016004, https://doi.org/10.3389/fphar.2022.1016004.

[5] H. Gong, X. Gan, Y. Li, et al., "Review on the Genus Polygonatum Polysaccharides: Extraction, Purification, Structural Characteristics and Bioactivities," *International Journal of Biological Macromolecules* 229 (2023): 909–930, https://doi.org/10.1016/j.ijbiomac.2022.12.320.

[6] S. Wang, G. Li, X. Zhang, et al., "Structural Characterization and Antioxidant Activity of Polygonatum Sibiricum Polysaccharides," *Carbohydrate Polymers* 291 (2022): 119524, https://doi.org/10.1016/j.carbpol.2022.119524.

[7] S. Xu, I. Ilyas, P. J. Little, et al., "Endothelial Dysfunction in Atherosclerotic Cardiovascular Diseases and Beyond: From Mechanism to Pharmacotherapies," *Pharmacological Reviews* 73, no. 3 (2021): 924–967, https://doi.org/10.1124/pharmrev.120.000096.

[8] S. Mu, Y. Xia, Q. Wu, et al., "Response of Bone Metabolism Markers to Ice Swimming in Regular Practitioners," *Frontiers in Physiology* 12 (2021): 731523, https://doi.org/10.3389/fphys.2021.731523.

[9] J. Su, Y. Wang, M. Yan, et al., "The Beneficial Effects of Polygonatum Sibiricum Red. Superfine Powder on Metabolic Hypertensive Rats via Gut-Derived LPS/TLR4 Pathway Inhibition," *Phytomedicine* 106 (2022): 154404, https://doi.org/10.1016/j.phymed.2022.154404.

[10] J. Wang, P. Chen, Q. Cao, W. Wang, and X. Chang, "Traditional Chinese Medicine Ginseng Dingzhi Decoction Ameliorates Myocardial Fibrosis and High Glucose-Induced Cardiomyocyte Injury by Regulating Intestinal Flora and Mitochondrial Dysfunction," *Oxidative Medicine and Cellular Longevity* 2022 (2022): 1–33, https://doi.org/10.1155/2022/9205908.

[11] M. Y. W. Ng, T. Wai, and A. Simonsen, "Quality Control of the Mitochondrion," *Developmental Cell* 56, no. 7 (2021): 881–905, https://doi.org/10.1016/j.devcel.2021.02.009.

[12] Z. Guan, J. Chen, L. Wang, et al., "Nuanxinkang Prevents the Development of Myocardial Infarction-Induced Chronic Heart Failure by Promoting PINK1/Parkin-Mediated Mitophagy," *Phytomedicine* 108 (2023): 154494, https://doi.org/10.1016/j.phymed.2022.154494.

[13] X. Li, S. Wei, S. Niu, et al., "Network Pharmacology Prediction and Molecular Docking-Based Strategy to Explore the Potential Mechanism of Huanglian Jiedu Decoction Against Sepsis," *Computers in Biology and Medicine* 144 (2022): 105389, https://doi.org/10.1016/j.compbiomed.2022.105389.

[14] A. Daina, O. Michielin, and V. Zoete, "SwissTargetPrediction: Updated Data and New Features for Efficient Prediction of Protein Targets of Small Molecules," *Nucleic Acids Research*

47, no. W1 (2019): W357–W364, https://doi.org/10.1093/nar/gkz382.

[15] D. Gfeller, A. Grosdidier, M. Wirth, A. Daina, O. Michielin, and V. Zoete, "SwissTargetPrediction: A Web Server for Target Prediction of Bioactive Small Molecules," *Nucleic Acids Research* 42, no. W1 (2014): W32–W38, https://doi.org/10.1093/nar/gku293.

[16] Y. Wang, Y. Yuan, W. Wang, et al., "Mechanisms Underlying the Therapeutic Effects of Qingfeiyin in Treating Acute Lung Injury Based on GEO Datasets, Network Pharmacology and Molecular Docking," *Computers in Biology and Medicine* 145 (2022): 105454, https://doi.org/10.1016/j.compbiomed.2022.105454.

[17] G. Yu, L. G. Wang, Y. Han, and Q. Y. He, "clusterProfiler: An R Package for Comparing Biological Themes Among Gene Clusters," *OMICS: A Journal of Integrative Biology* 16, no. 5 (2012): 284–287, https://doi.org/10.1089/omi.2011.0118.

[18] H. M. Berman, J. Westbrook, Z. Feng, et al., "The Protein Data Bank," *Nucleic Acids Research* 28, no. 1 (2000): 235–242, https://doi.org/10.1093/nar/28.1.235.

[19] W. Pan, W. Li, H. Wu, et al., "Aging-Accelerated Mouse Prone 8 (SAMP8) Mice Experiment and Network Pharmacological Analysis of Aged Liupao Tea Aqueous Extract in Delaying the Decline Changes of the Body," *Antioxidants* 12, no. 3 (2023): 685, https://doi.org/10.3390/antiox12030685.

[20] Y. Xie, Z. Jiang, R. Yang, et al., "Polysaccharide-Rich Extract From Polygonatum Sibiricum Protects Hematopoiesis in Bone Marrow Suppressed by Triple Negative Breast Cancer," *Biomedicine & Pharmacotherapy* 137 (2021): 111338, https://doi.org/10.1016/j.biopha.2021.111338.

[21] W. Ma, S. Wei, W. Peng, et al., "Antioxidant Effect of Polygonatum Sibiricum Polysaccharides in D-Galactose-Induced Heart Aging Mice," *BioMed Research International* 2021, no. 1 (2021): 6688855, https://doi.org/10.1155/2021/6688855.

[22] S. B. Du, H. H. Zhou, P. F. Wang, et al., "Modulation Effects of Danshen-Honghua Herb Pair on Gut Microbiota of Acute Myocardial Ischemia Model Rat," *FEMS Microbiology Letters* 369, no. 1 (2022): fnac036, https://doi.org/10.1093/femsle/fnac036.

[23] Z. Ke, G. Wang, L. Yang, et al., "Crude Terpene Glycoside Component From Radix Paeoniae Rubra Protects Against Isoproterenol-Induced Myocardial Ischemic Injury via Activation of the PI3K/AKT/mTOR Signaling Pathway," *Journal of Ethnopharmacology* 206 (2017): 160–169, https://doi.org/10.1016/j.jep.2017.05.028.

[24] C. Liu, B. Li, Q. Yan, et al., "Protective Effects and Mechanisms of Recombinant Human Glutathione Peroxidase 4 on Isoproterenol-Induced Myocardial Ischemia Injury," *Oxidative Medicine and Cellular Longevity* 2021, no. 1 (2021): 6632813, https://doi.org/10.1155/2021/6632813.

[25] Y. Hu, X. Wang, Q. Li, Y. Pan, and L. Xu, "Salvianolic Acid B Alleviates Myocardial Ischemic Injury by Promoting Mitophagy and Inhibiting Activation of the NLRP3 Inflammasome," *Molecular Medicine Reports* 22, no. 6 (2020): 5199–5208, https://doi.org/10.3892/mmr.2020.11589.

[26] M. I. Ahmed, H. M. A. Abdelrazek, Y. M. Moustafa, et al., "Cardioprotective Effect of Flibanserin Against Isoproterenol-Induced Myocardial Infarction in Female Rats: Role of Cardiac 5-HT2A Receptor Gene/5-HT/Ca^{2+} Pathway," *Pharmaceuticals* 16, no. 4 (2023): 502, https://doi.org/10.3390/ph16040502.

[27] H. Yu, B. Chen, and Q. Ren, "Baicalin Relieves Hypoxia-Aroused H9c2 Cell Apoptosis by Activating Nrf2/HO-1-Mediated HIF1α/BNIP3 Pathway," *Artificial Cells, Nanomedicine, and Biotechnology* 47, no. 1 (2019): 3657–3663, https://doi.org/10.1080/21691401.2019.1657879.

[28] B. Zhao, G. P. Li, J. J. Peng, et al., "Schizandrin B Attenuates Hypoxia/Reoxygenation Injury in H9c2 Cells by Activating the AMPK/Nrf2 Signaling Pathway," *Experimental and Therapeutic Medicine* 21, no. 3 (2021): 220, https://doi.org/10.3892/etm.2021.9651.

[29] L. Qiu, Q. Zhao, L. Dai, et al., "Long Non-Coding RNA DANCR Alleviates Hypoxia-Caused H9c2 Cells Damage Through Up Regulation of HIF-1α," *Artificial Cells, Nanomedicine, and Biotechnology* 48, no. 1 (2020): 533–541, https://doi.org/10.1080/21691401.2020.1725026.

[30] J. Shi, T. Yu, K. Song, et al., "Dexmedetomidine Ameliorates Endotoxin-Induced Acute Lung Injury In Vivo and In Vitro by Preserving Mitochondrial Dynamic Equilibrium Through the HIF-1a/HO-1 Signaling Pathway," *Redox Biology* 41 (2021): 101954, https://doi.org/10.1016/j.redox.2021.101954.

[31] W. Rong, J. Li, L. Wang, et al., "Investigation of the Protective Mechanism of Leonurine Against Acute Myocardial Ischemia by an Integrated Metabolomics and Network Pharmacology Strategy," *Frontiers in cardiovascular medicine* 9 (2022): 969553, https://doi.org/10.3389/fcvm.2022.969553.

[32] J. Y. Hou, G. Z. Cao, L. L. Tian, et al., "Integrated Transcriptomics and Metabolomics Analysis Reveals That C3 and C5 Are Vital Targets of DuZhi Wan in Protecting Against Cerebral Ischemic Injury," *Biomedicine & Pharmacotherapy* 155 (2022): 113703, https://doi.org/10.1016/j.biopha.2022.113703.

[33] A. Pilipović, D. Mitrović, S. Obradović, and M. Poša, "Docking-Based Analysis and Modeling of the Activity of Bile Acids and Their Synthetic Analogues on Large Conductance Ca^{2+} Activated K Channels in Smooth Muscle Cells," *European Review for Medical and Pharmacological Sciences* 25, no. 23 (2021): 7501–7507, https://doi.org/10.26355/eurrev_202112_27449.

[34] J. Lehmacher, J. T. Neumann, N. A. Sörensen, et al., "Predictive Value of Serial ECGs in Patients With Suspected Myocardial Infarction," *Journal of Clinical Medicine* 9, no. 7 (2020): 2303, https://doi.org/10.3390/jcm9072303.

[35] X. Zhang, Q. Du, Y. Yang, et al., "The Protective Effect of Luteolin on Myocardial Ischemia/Reperfusion (I/R) Injury Through TLR4/NF-Kb/nlrp3 Inflammasome Pathway," *Biomedicine & Pharmacotherapy* 91 (2017): 1042–1052, https://doi.org/10.1016/j.biopha.2017.05.033.

[36] M. Liu, P. Liu, B. Zheng, et al., "Cardioprotective Effects of Alantolactone on Isoproterenol-Induced Cardiac Injury and Cobalt Chloride-Induced Cardiomyocyte Injury," *International Journal of Immunopathology and Pharmacology* 36 (2022): 20587384211051993, https://doi.org/10.1177/20587384211051993.

[37] Z. Wang, F. Zhang, W. Liu, N. Sheng, H. Sun, and J. Zhang, "Impaired Tricarboxylic Acid Cycle Flux and Mitochondrial Aerobic Respiration During Isoproterenol Induced Myocardial Ischemia Is Rescued by Bilobalide," *Journal of pharmaceutical analysis* 11, no. 6 (2021): 764–775, https://doi.org/10.1016/j.jpha.2020.08.008.

[38] L. Liang, F. Sun, H. Wang, and Z. Hu, "Metabolomics, Metabolic Flux Analysis and Cancer Pharmacology," *Pharmacology & Therapeutics* 224 (2021): 107827, https://doi.org/10.1016/j.pharmthera.2021.107827.

[39] Y. Zhou, X. Feng, H. Xu, et al., "The Application of Natural Product-Delivering Micro/Nano Systems in the Treatment of Inflammatory Bowel Disease," *Journal of Materials Chemistry B* 11, no. 2 (2023): 244–260, https://doi.org/10.1039/d2tb01965e.

[40] Y. Jiang, "Osteoarthritis Year in Review 2021: Biology," *Osteoarthritis and Cartilage* 30, no. 2 (2022): 207–215, https://doi.org/10.1016/j.joca.2021.11.009.

[41] J. Zheng, P. Chen, J. Zhong, et al., "HIF-1α in Myocardial Ischemia-Reperfusion Injury (Review)," *Molecular Medicine Reports* 23, no. 5 (2021): 352, https://doi.org/10.3892/mmr.2021.11991.

[42] X. X. Lai, N. Zhang, L. Y. Chen, et al., "Latifolin Protects Against Myocardial Infarction by Alleviating Myocardial Inflammatory via the HIF-1α/NF-κB/IL-6 Pathway," *Pharmaceutical Biology* 58, no. 1 (2020): 1165–1175, https://doi.org/10.1080/13880209.2020.1840597.

[43] S. Yuan, C. Wei, G. Liu, et al., "Sorafenib Attenuates Liver Fibrosis by Triggering Hepatic Stellate Cell Ferroptosis via HIF-1α/SLC7A11 Pathway," *Cell Proliferation* 55, no. 1 (2022): e13158, https://doi.org/10.1111/cpr.13158.

[44] K. Keylani, F. Arbab Mojeni, A. Khalaji, et al., "Endoplasmic Reticulum as a Target in Cardiovascular Diseases: Is There a Role for Flavonoids?" *Frontiers in Pharmacology* 13 (2022): 1027633, https://doi.org/10.3389/fphar.2022.1027633.

[45] Y. Jiang, D. Wang, K. Wu, et al., "Cloning and Characterization of the Gene Encoding HMGS Synthase in Polygonatum Sibiricum," *BioMed Research International* 2022, no. 1 (2022): 7441296, https://doi.org/10.1155/2022/7441296.

[46] S. Huang, H. Yuan, W. Li, et al., "Polygonatum Sibiricum Polysaccharides Protect Against MPP-Induced Neurotoxicity via the Akt/mTOR and Nrf2 Pathways," *Oxidative Medicine and Cellular Longevity* 2021, no. 1 (2021): 8843899, https://doi.org/10.1155/2021/8843899.

[47] A. C. Leite, V. Costa, and C. Pereira, "Mitochondria and the Cell Cycle in Budding Yeast," *The International Journal of Biochemistry & Cell Biology* 161 (2023): 106444, https://doi.org/10.1016/j.biocel.2023.106444.

[48] C. Han, Y. Zhu, Z. Yang, S. Fu, W. Zhang, and C. Liu, "Protective Effect of Polygonatum Sibiricum Against Cadmium-Induced Testicular Injury in Mice through Inhibiting Oxidative Stress and Mitochondria-Mediated Apoptosis," *Journal of Ethnopharmacology* 261 (2020): 113060, https://doi.org/10.1016/j.jep.2020.113060.

[49] X. F. Yang, Y. Miao, D. W. Yang, et al., "UPLC-Q TOF-MS-Based Metabolomics and Anti-Myocardial Ischemia Activity of Dioscoreae Nipponicae Rhizoma From Different Geographical Origins," *Journal of Pharmaceutical and Biomedical Analysis* 234 (2023): 115551, https://doi.org/10.1016/j.jpba.2023.115551.

[50] G. Luo, J. Lin, W. Cheng, Z. Liu, T. Yu, and B. Yang, "UHPLC-Q-Orbitrap-MS-Based Metabolomics Reveals Chemical Variations of Two Types of Rhizomes of Polygonatum Sibiricum," *Molecules* 27, no. 15 (2022): 4685, https://doi.org/10.3390/molecules27154685.